



Memorandum

U.S. Department
of Transportation

**National Highway
Traffic Safety
Administration**

Subject: Motorcoach Safety Research

Date: OCT 27 2010

From: David Sutula
Safety Standards Engineer *DS*

Reply to
Attn of:

To: Docket No. NHTSA-2007-28793

Thru: Lori Summers *Lori Summers*
Acting Director, Office of Crashworthiness Standards

O. Kevin Vincent
Chief Counsel

Dorothy R. Nakama for

OCT. 27, 2010

Attached is a report titled, "Motorcoach Flammability Project Interim Report: Tire Fire Penetration into the Passenger Compartment," prepared by the National Institute of Standards and Technology. This report presents the results of the first year of a two-year NHTSA-funded research effort to address fire safety issues related to motorcoaches and other elements of Federal Motor Vehicle Safety Standard (FMVSS) No. 302, "Flammability of interior materials."

This interim report describes two experiments that were conducted using a bus mock-up designed to imitate fires that initiate through frictional heating of hub and wheel metal caused by failed axle bearings, locked brakes, or dragged blown tires. Measurements of interior and exterior temperatures, interior heat flux, and heat release rates were performed. Both experiments showed that fires initiating in the rear wheel well area ignited the glass-reinforced plastic exterior side panels (below the windows) upon which the fires spread quickly and penetrated the passenger compartment through the heat-affected broken windows.

Attachment

NIST Technical Note 1653

**Motorcoach Flammability Project
Interim Report: Tire Fire Penetration
into the Passenger Compartment**

Erik L. Johnsson
Jiann C. Yang

NIST Technical Note 1653

**Motorcoach Flammability Project
Interim Report: Tire Fire Penetration
into the Passenger Compartment**

Erik L. Johnsson
Jiann C. Yang
*Building and Fire Research Laboratory
National Institute of Standards and Technology*

April 2010



U.S. Department of Commerce
Gary Locke, Secretary

National Institute of Standards and Technology
Patrick D. Gallagher, Director

Certain commercial entities, equipment, or materials may be identified in this document in order to describe an experimental procedure or concept adequately. Such identification is not intended to imply recommendation or endorsement by the National Institute of Standards and Technology, nor is it intended to imply that the entities, materials, or equipment are necessarily the best available for the purpose.

TABLE OF CONTENTS

ABSTRACT.....	iv
INTRODUCTION	1
EXPERIMENTAL SET-UP	3
Experimental Preparation.....	3
Obtaining the Motorcoach	3
Moving and Securing the Motorcoach.....	3
Straightening Window Posts.....	3
Removing Unsafe Materials	7
Replacement Components	7
Burner	7
Measurement Instrumentation	10
Total and Burner Heat Release Rates	10
Temperature	10
Heat Flux.....	15
Image Recording.....	18
Standard and Infrared Video.....	18
Still Photography	20
General Procedures	20
RESULTS AND DISCUSSION	22
Event Timing	22
Heat Release Rate	24
Wheel, Tire, and Wheel Well Temperatures	26
Window and Panel Temperatures	29
Floor, Lavatory, and Central Tunnel Temperatures.....	34
Axle Temperatures.....	38
Heat Fluxes	40
Photographs.....	42
SUMMARY AND OBSERVATIONS.....	42
ACKNOWLEDGEMENTS	43
REFERENCES	44
APPENDICES	45
Appendix A. Motorcoach Flammability Testing Statement of Work (SOW).....	45
Appendix B. Channel description and hook-up list.....	52
Appendix C. Photographs	57

ABSTRACT

Two full scale fire experiments were conducted to determine the mode of penetration of a tire fire into the passenger compartment of a motorcoach. A burner was designed to imitate the frictional heating of hub and wheel metal caused by failed axle bearings, locked brakes, or dragged blown tires. For the first experiment, heating to obtain tire ignition was initiated on the exterior of the passenger side tag axle wheel and for the second, on the exterior of the passenger side drive axle wheel. Measurements of interior and exterior temperatures, interior heat flux, and heat release rate were performed. Also, standard and infrared videos and still photographs were recorded. Both experiments showed that the tire fires ignited the plastic fender and glass-reinforced plastic (GRP) exterior side panel (below the windows) upon which the fires spread quickly and penetrated the passenger compartment by breaking the windows. Measurements showed that other potential fire penetration routes (flooring and lavatory) lagged far behind the windows in heating and degradation.

KEYWORDS

Motorcoach fire, bus fire, tire fire, vehicle fire, window breakage, fire penetration

INTRODUCTION

Research of vehicle fires is important for the prevention of life and property losses. While death by fire in a burning vehicle is a tragedy, fires in vehicles such as motorcoaches which carry as many as 56 passengers are especially tragic as they impact whole communities, regions, or a nation. One such fire occurred during the evacuation of Gulf Coast residents during Hurricane Rita in 2005. On September 23, 2005, near Wilmer, TX, a motorcoach carrying nursing home residents experienced a failed right bearing on the tag axle resulting in a tire fire which spread to consume the motorcoach. Twenty-three occupants died because many were not mobile and could not escape the motorcoach before being overcome by smoke and flames. [1] Even when there are no fatalities in motorcoach or bus fires, complete loss of the coach and passenger property is typical. [2]

The National Highway Traffic Safety Administration (NHTSA) has sponsored the National Institute of Standards and Technology (NIST) to conduct research to support NHTSA's current effort on improving motorcoach fire safety based on recent National Transportation Safety Board (NTSB) recommendations. The pertinent recommendations were:

H-07-05: Develop a Federal Motor Vehicle Safety Standard to provide fire-hardening of exterior fire-prone materials, such as those in areas around wheel-wells, to limit the potential for flame spread into a motorcoach or bus passenger compartment.

H-07-06: Develop detection systems to monitor the temperature of wheel-well compartments in motorcoaches and buses to provide early warning of malfunctions that could lead to fires.

The research will:

- Establish an understanding of the development of a motorcoach fire and its subsequent spread into the passenger compartment.
- Evaluate and identify bench-scale material flammability test methods that are most likely to give a meaningful measure of the resistance of interior materials of a motorcoach to a typical wheel-well fire.
- Determine the feasibility of establishing requirements for fire-hardening or fire resistance of motorcoach exterior components, including fuel system components.
- Assess tenability within the passenger compartment in the event of a wheel-well fire and identify potential mitigation strategies.

Appendix A contains a more detailed statement of work (SOW) for the overall project. The SOW was planned to accomplish the above objectives. The research described here is related only to the first bullet on the list. Whereas motorcoach fires may result from electrical system shorts, engine compartment leaks, component overheating, or tire fires, this research was focused on the penetration of motorcoach *tire fires* into the passenger compartment. The causes of tire fires (failed axle bearings, locked brakes, or dragged blown tires) are common to all makes and models of motorcoaches. [2]

There is a small body of previous research related to vehicle fires, motorcoach fires, and tire fires at the Scandinavian research institutes. Hansen at the Norwegian Fire Research Laboratory (SINTEF NBL) focused on tire fire experiments as related to vehicles in general, but not buses in particular. [3] Hammarström et al. at SP Technical Research Institute of Sweden (SP) studied major fire causes in buses. [4] A more recent, follow-up paper from SP provided an overview of the entire bus fire problem and included the results of full scale bus experiments. [5]

For the NIST research project, only the rear half of a motorcoach was used. Two full scale fire experiments were performed. In order to imitate the frictional heating of hub and wheel metal caused by failed axle bearings, locked brakes, or dragged blown tires, a unique burner was designed to only heat the metal of the wheel without preheating the tire rubber. Each experiment was ignited by heating a different wheel. The first started on the passenger side (right side when facing forward) tag (rearmost, also called dead or lazy) axle, which only had one wheel and tire per side. This experiment most closely emulated the Hurricane Rita evacuation motorcoach tire fire. The second experiment started on the passenger side drive axle (in front of the tag axle), which had two wheels and tires per side.

For each tire fire experiment, temperature measurements were made and recorded of the interior near the windows and on the floor, of the exterior near the windows and body panels, on the wheels and tires, and in the wheel well and axle regions. Interior heat fluxes were measured in several locations, and the total heat release rate of the fire was calculated from the hood exhaust using oxygen depletion calorimetry. Standard and infrared videos and still photographs were recorded.

EXPERIMENTAL SET-UP

Experimental Preparation

Obtaining the Motorcoach

The motorcoach used for these experiments was a Motor Coach Industries model 102EL3 which is the same model as the one which burned near Wilmer, TX, during the Hurricane Rita evacuation. This model has a capacity of 55 passengers, includes a lavatory, has a mass of approximately 17 000 kg (38 000 lb) empty, and has a 13.92 m (45.7 ft) length, 2.59 m (8.5 ft) width, and 3.59 m (11.77 ft) height. Initially, the motorcoach was employed in a front-end crash test in Ohio. Damage to the rear half of the motorcoach was minor and expected to have negligible effect on the tire fire experiments. A specialist at cutting motorcoaches was brought in to cut the motorcoach approximately in half using multiple types of saws. Undamaged or intact components from the crashed front of the motorcoach, such as exterior glass reinforced plastic (GRP) panels, windows, seats, luggage racks, and trim panels, were salvaged and secured in the rear of the bus. The bus was transported to the Large Fire Laboratory (LFL) at the NIST campus in Maryland, where a large fork lift was used to unload and park the motorcoach. Figure 1 is a drawing which shows the rear half of the motorcoach with labels and dimensions of the most important components. Expanded uncertainties on the measured dimensions are estimated to be ± 3 mm. The width of the interior floor (not shown) was 2.44 m.

Moving and Securing the Motorcoach

A large forklift was used to transfer the motorcoach to the high-bay experimental area in the LFL with the steering assistance of another forklift. The larger forklift generally pushed the motorcoach from the rear to prevent it from dragging on the ground. The motorcoach was able to roll on its own six tires. Once the test section was safely transported to the designated anchoring area underneath the hood, it was secured with the undercarriage approximately 30 cm above the floor (above protective gypsum panels) on wooden cribbing [multiple 15 cm (6 in) by 15 cm (6 in) timber beams and smaller pieces of wood]. Figure 2 is a photograph of some of the cribbing used to support the motorcoach during testing. The lifting and securing was accomplished with jacks and jack stands.

Straightening Window Posts

During the crash test, the roof was pushed backward between 7 cm and 10 cm. The window posts were angled back with the tops behind the bottoms which created non-rectangular window openings preventing window closure. To straighten the posts and maintain the latching mechanisms in the centers of the window openings, the tops of the posts were cut completely and the bottoms were notched on 3 sides to enable the top to be bent towards the front. In the new vertical positions, the posts were reattached to the roof with self tapping screws. Figure 3 shows photographs of the cutting operation, notched post, and reattachment.

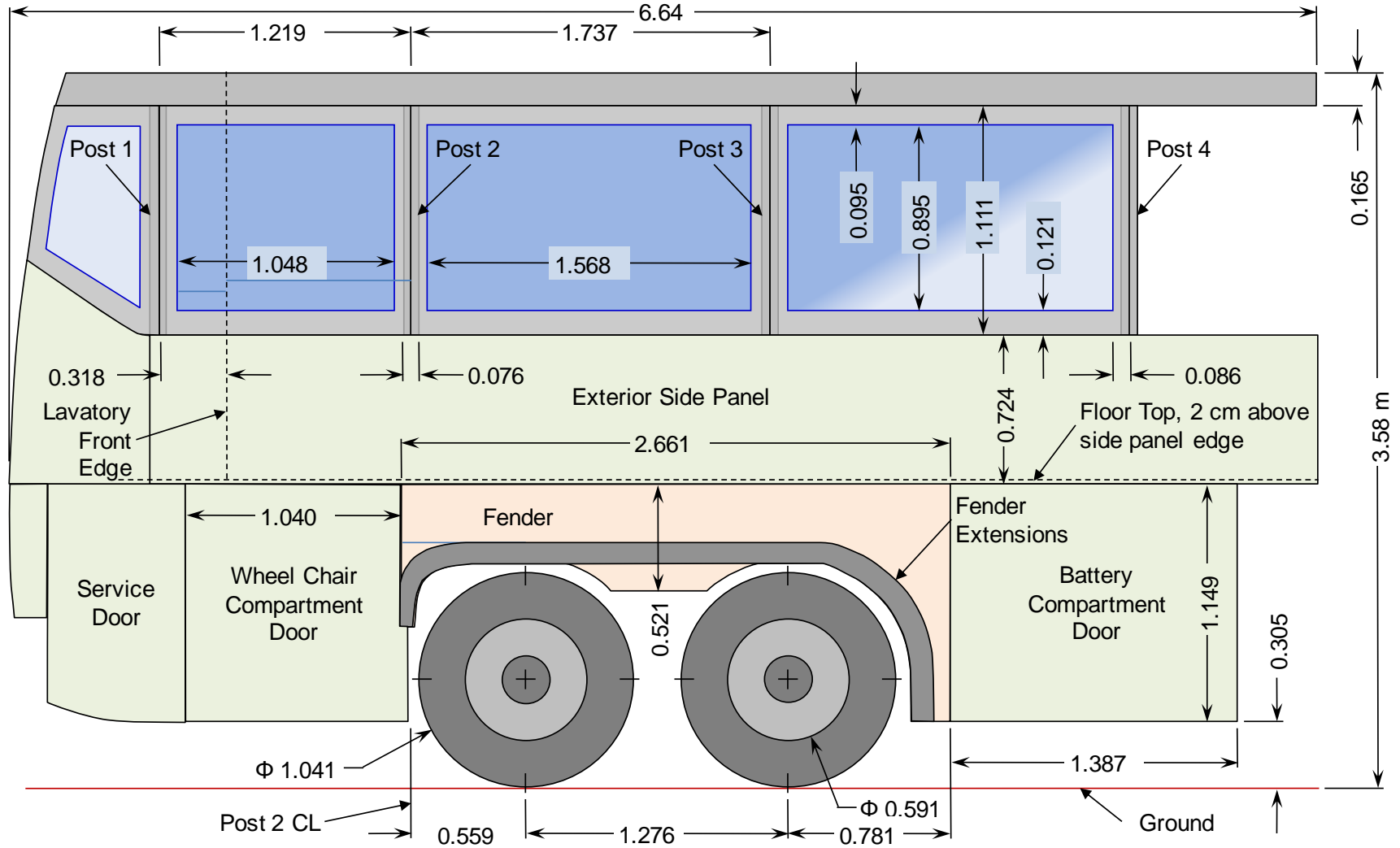


Figure 1 A drawing of the motorcoach rear half which was used for tire fire experiments. Dimensions are in meters. Distance measurement uncertainty is ± 3 mm.



Figure 2 A photograph of the cribbing supporting the motorcoach during testing.

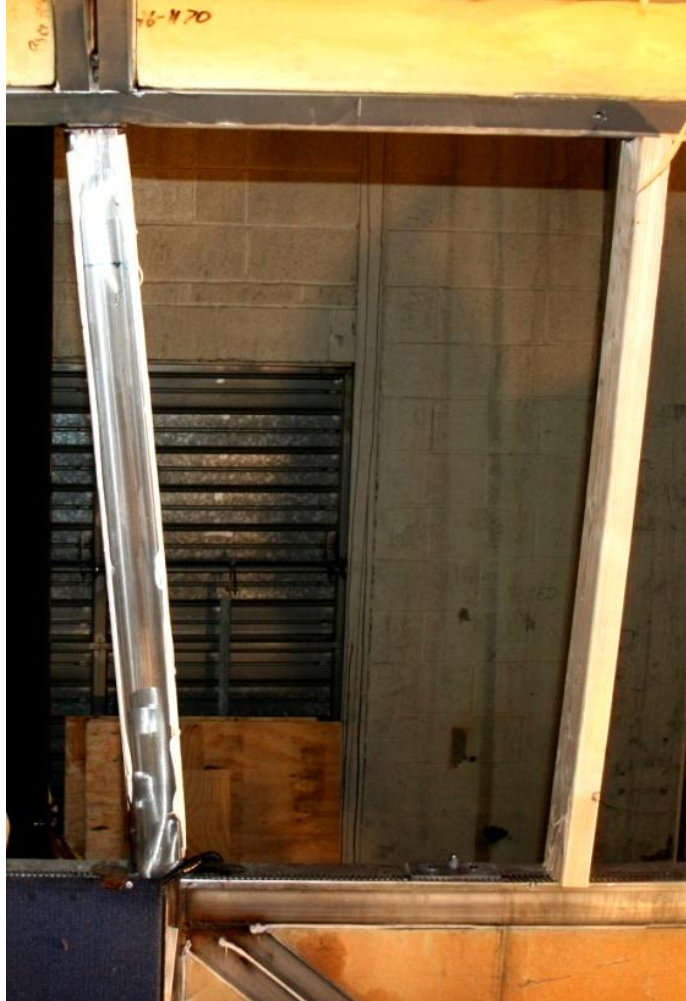


Figure 3 Window post straightening operation. The top photograph shows the original angle of a bent post. The bottom right photograph shows the notch at the bottom of the post. The bottom left photograph shows the angle bracket with self-tapping screws which reattached the roof to the post.

Removing Unsafe Materials

Safety being paramount, motorcoach components that might prove dangerous during the fire experiments were removed or made safe. The tires were deflated and then cut so they could not burst under pressure. The coach was supported by the cribbing under the frame and axles and not by the tires during testing. The batteries and the fuel tank were removed. Pressurized air and nitrogen tanks for the pneumatic and other systems were removed or punctured. Coolant, transmission, hydraulic, and brake fluids were drained from their systems.

Replacement Components

For the second experiment, fire damaged parts of the motorcoach were replaced. Wheels [aluminum, 57 cm (22.5 in) diameter by 23 cm (9.00 in) wide], tires (315/80R22.5), and long side windows were replaced with non-fire-exposed replacements. The exterior side panel was replaced with the front right portion salvaged from the front of the motorcoach. A new short right side window, and new fender and fender trim were purchased from the manufacturer. Installation of the fender and exterior panel generally followed the maintenance manual for the motorcoach and some off the shelf comparable sealants and fasteners.

Burner

A special burner was designed and built that would direct substantial heat, (up to 100 kW) on the metal of a motorcoach wheel without the flames or exhaust gases impinging on the rubber. The purpose of this design was to cause the rubber to ignite just from heat conduction with hot metal, which qualitatively simulates the frictional heat generated from failed axle bearings, locked brakes, and dragged blown tires.

The design of the burner was a circular 25 mm outer diameter stainless steel (type 304) tube with 10 high output heating torch nozzles attached perpendicular to the plane of the circular tube. Figure 4 shows a schematic of this design. A purchased assembly of valves and a mixing chamber for the natural gas and high-pressure air was attached to the circular tube. The flames were meant to be pre-mixed so nearly all of the heat was efficiently generated at the flames. Flame arresting torch tips were used. The burner was designed with the requirement of a heat output between 50 kW and 100 kW based on a calculation using an estimate of the total mass of the wheel and associated metal and a target heating duration between 30 min and 1 h.

The burner was mounted on a long, wheeled cart to enable positioning of the flame tips and fast removal of the burner after tire ignition. A tire shield was fabricated and placed between the wheel and tire to prevent direct heating of the tire by burner flames and gases. For the second test, a calcium silicate blanket was placed on top of the shield for additional insulation to minimize radiation and convection from the shield to the tire. Figure 5 shows photographs of the burner and shield.

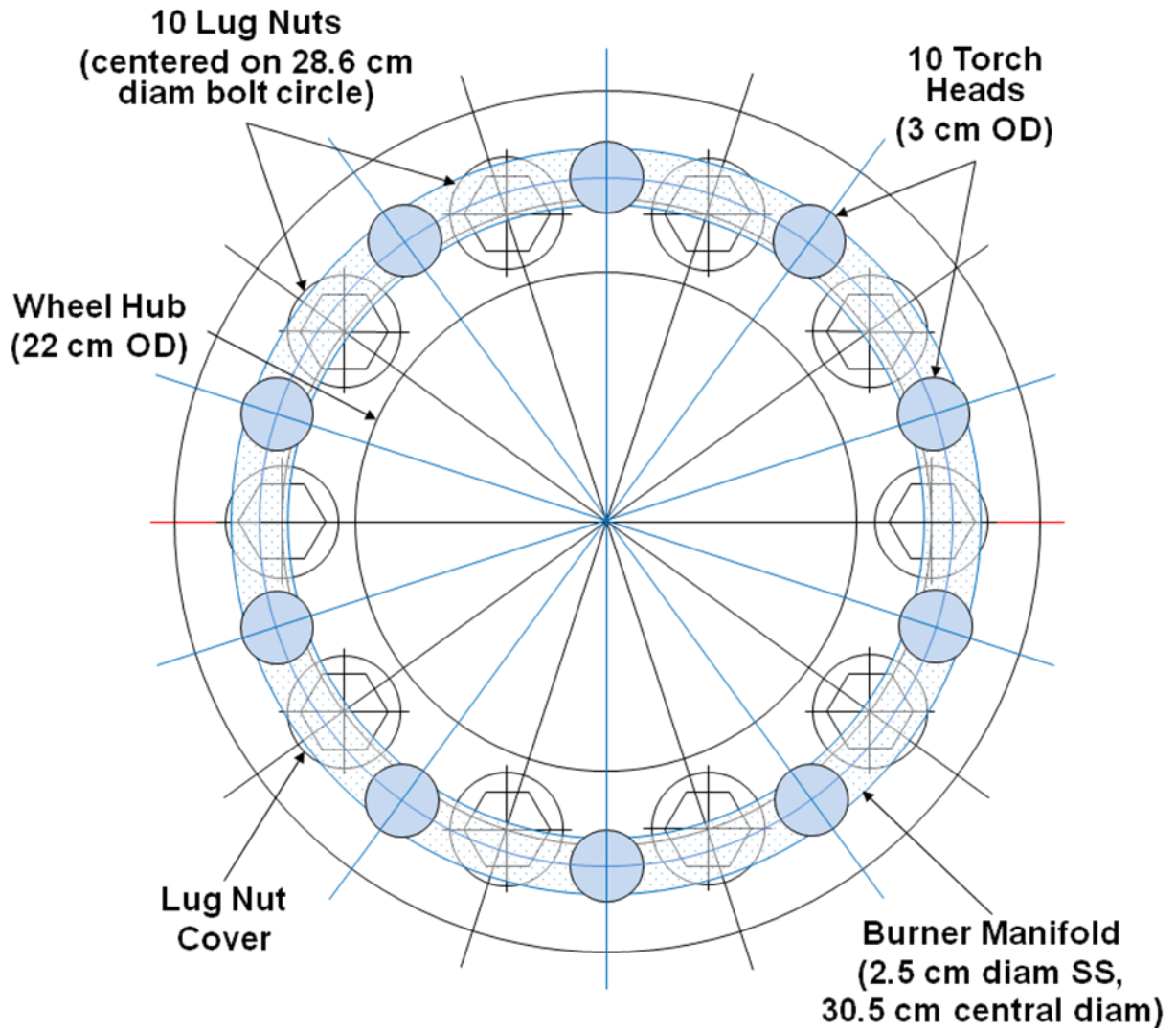


Figure 4 A schematic of the wheel burner design showing the relative locations of the 10 torch heads and manifold compared to the wheel's hub, lug nuts, and lug nut covers. The outer circle represents the wheel's curvature away from the lug nut surface plane.

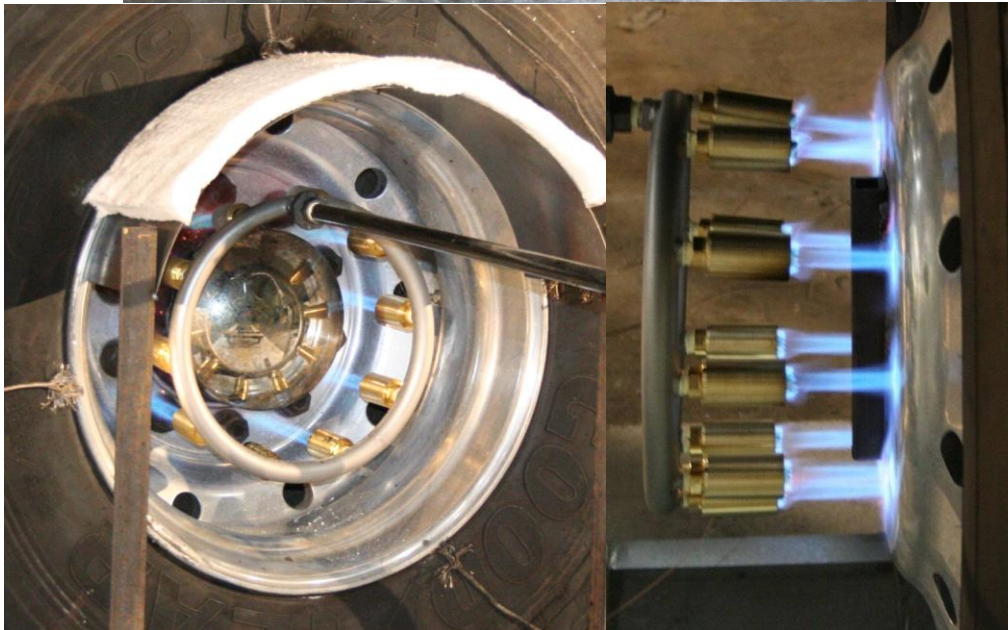
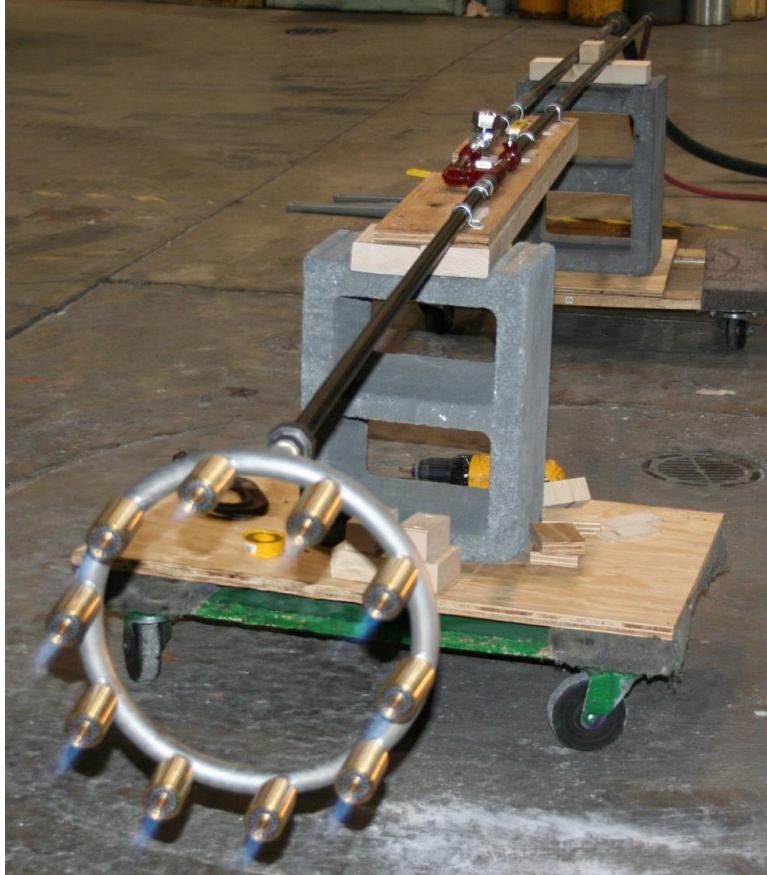


Figure 5 The burner for heating the wheels. The top photograph shows the whole assembly including the burner ring, wheeled cart, and gas and air valves. The bottom right photograph shows the pre-mixed natural gas and air torches impinging on a tag axle wheel. The bottom left photograph shows the tire shield nested inside a drive axle wheel rim with an insulating cover to minimize convective and radiative heating to the tire from the shield.

Measurement Instrumentation

Measurements of heat release rate, heat fluxes, and interior and exterior temperatures were recorded for each experiment. The details of the types of measurements and locations are described below. A data acquisition system (DAQ), described in [6], was used to record 151 channels of sensor output voltages every second. Each voltage was the average of 200 readings scanned each second. This DAQ was separate from that used for the calorimetry system described below.

Total and Burner Heat Release Rates

The total heat release rate (HRR) was measured using oxygen depletion calorimetry. Details of the constituent measurements and calculations can be found in [6]. The experiments were performed under the NIST Large Fire Laboratory (LFL) 9 m by 12 m hood which utilizes up to two fan trains, each of which can be set to a maximum flow of about 21 m³/s (45 000 ft³/min). The LFL exhaust hood is capable of capturing the smoke from a steady 10 MW fire and transients up to 30 MW over periods less than 15 s. Calibrations of the hood up to 8 MW are performed with metered natural gas fires. The calorimeter combined expanded uncertainty for natural gas was about $\pm 7.6\%$ based on a natural gas calibration burner test performed two weeks before the motorcoach experiments. That uncertainty was calculated over the whole range of the calorimeter's operation. Uncertainties in a narrow range, for example around 1 MW as for these fires, can be much lower. Since the motorcoach experiments involved an unknown mixture of fuels, the expanded uncertainty increases by 5% (in quadrature) to 9.1%. The increased uncertainty is from an empirical constant for heat released per mole of oxygen consumed for a range of hydrocarbon fuels. [7]

The flow of natural gas to the burner was measured with the DAQ of the calorimeter for an accurate and independent calculation of ideal (assumed 100% efficient) HRR solely related to the burner. The burner HRR expanded uncertainty was calculated to be $\pm 2.5\%$ for the 60 kW level at which it operated for these experiments.

Temperature

Temperatures were measured on and around the wheels and tires, along the exterior panel and windows, and inside the motorcoach along the windows and on the floor. K-type thermocouples (TCs) were used throughout. For locations where flames were expected such as near the heated wheels and over the exterior panel and windows, special Nextel (ceramic fiber) insulation was used while the rest had a fiberglass braid. The numbers of temperature measurements at specific locations are listed in Table 1. Additional descriptions of the locations are in the channel description and instrument hook-up list which is provided in Appendix B. The channel descriptions also provide a key to measurement label names used in the plots. Thermocouples were attached to the floor with staples, and the beads were bent to touch the surface. Wheel TCs were secured with screws and washers and tire TCs were held in place with screws. Figure 6 shows the locations of the tire and wheel TCs. The locations are labeled with the same scheme used in the channel list (Appendix B) and temperature plots.

The uncertainties associated with the gas and surface temperature measurements away from the fire were approximately ± 2 °C.[6] For thermocouples impinged by fire, the gas temperatures recorded may be as much as 10 % (90 °C) low for a 600 °C reading and 20 % (220 °C) low for a 850 °C reading. [8] These offsets are due to radiative heat losses from the thermocouple beads to the relatively cold surroundings. Uncertainties of surface temperatures for thermocouples exposed to fire were estimated to be approximately ± 10 °C. The main purposes of the temperature measurements were to monitor progress of the tires toward ignition and identify relatively hotter locations generated by the tire fire in and around the motorcoach. The uncertainties in the temperature measurements were not detrimental to either of these purposes. Expanded uncertainty on thermocouple locations is about ± 1 cm.

Table 1 Numbers of thermocouples and location descriptions

General Location	Specific Location	Number of TCs
Wheels	Heated wheel on back side in a plus pattern, 0°, 90°, 180°, and 270° from top	4
Tires	Heated tire on front side between wheel rim and tire in plus pattern, 0°, 90°, 180°, and 270° from top	4
Wheel well	Rearmost corner of wheel well, over center of rear (tag axle) wheel, above center between wheels, over center of front (drive axle) wheel, and at front most corner of wheel well.	5
Above axles	Left, center, and right above each axle.	6
Outside windows and exterior panel	In a grid with 38 cm spacing consisting of 12 columns and 4 rows. Bottom row over exterior panel, other rows over windows.	48
Inside windows and in space above	In a grid with (generally) 38 cm spacing consisting of 12 columns and 4 rows. Bottom 3 rows over windows, top row in space above window 17 cm above top window row.	48
Interior floor	Along fire-side wall aligned with wheel well TCs with extra 46 cm behind rearmost and 46 cm in front of front most	7
	Along outside and inside of lavatory wall joint with floor	3
	In central cable tunnel under center of floor aligned with the rear most, center, and front most interior TCs at the side wall.	3

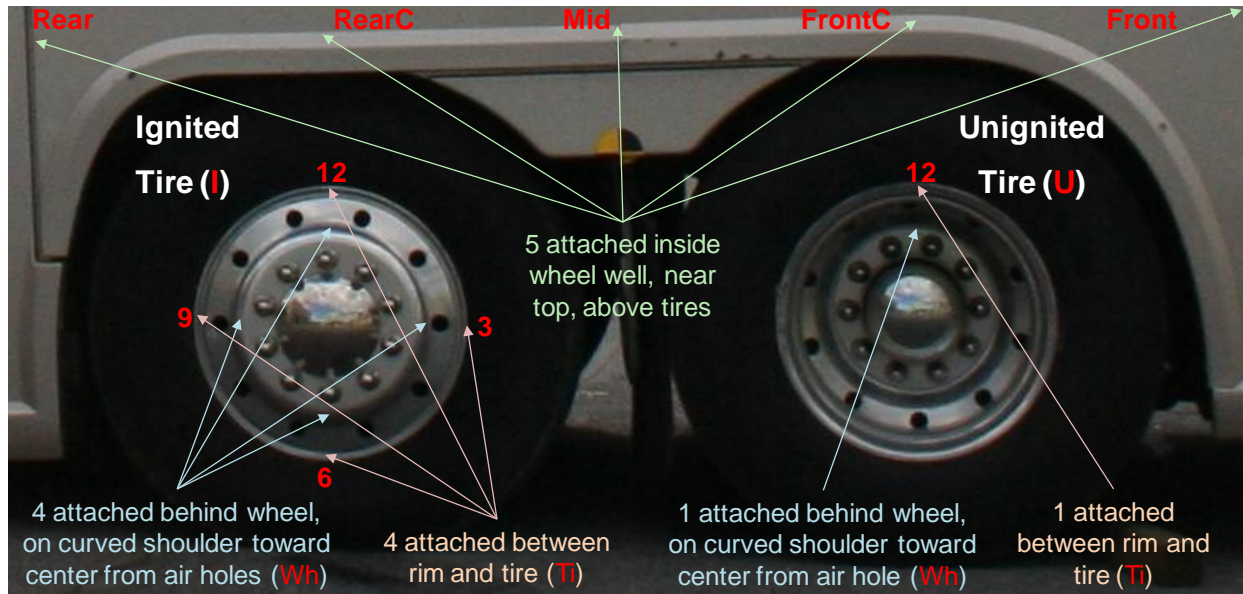


Figure 6 A photograph of the passenger side wheel well area with the locations of thermocouples shown for the tag axle wheel experiment. The ignited and unignited tires (and their thermocouples) were reversed for the drive axle experiment. Labels (in red) are used in temperature plot legends.

The exterior window and panel thermocouples were spaced 38 cm apart (vertically and horizontally) in 12 columns of 4 rows each for a total of 48 measurements. Three of the rows were over the glass while the bottom row was over the panel. Thermocouples were placed about 1 cm from the window surface. Figure 7 (top) shows a diagram with the spacing of the thermocouples and locations relative to the windows and posts. The diagram shows that the gap between columns of thermocouples and adjacent window posts was about 2.4 cm, and the gap between the bottom window row and the bottom of the window was about 3 cm. Figure 7 (bottom) is a photograph of the grid of exterior thermocouples as installed.

For the interior thermocouples near the windows, the spacing was generally the same as the exterior, and over the window area, both interior and exterior thermocouples were aligned on the same grid. The interior grid of thermocouples was shifted upward by one row so that the bottom row was over glass, and the top row was above the window in the space below the parcel rack. That top interior row was spaced only 17 cm above the top window row as the only exception to the 38 cm spacing. Figure 8 shows a diagram of the interior grid spacing. As on the exterior, the distance of the thermocouples from the glass was about 1 cm.

The approximate locations of interior floor thermocouples are depicted in Figure 9. The diagram differentiates those near the wall under the windows, those along the lavatory wall and door, and those under the floor in the central tunnel. The locations are further described in Table 1.

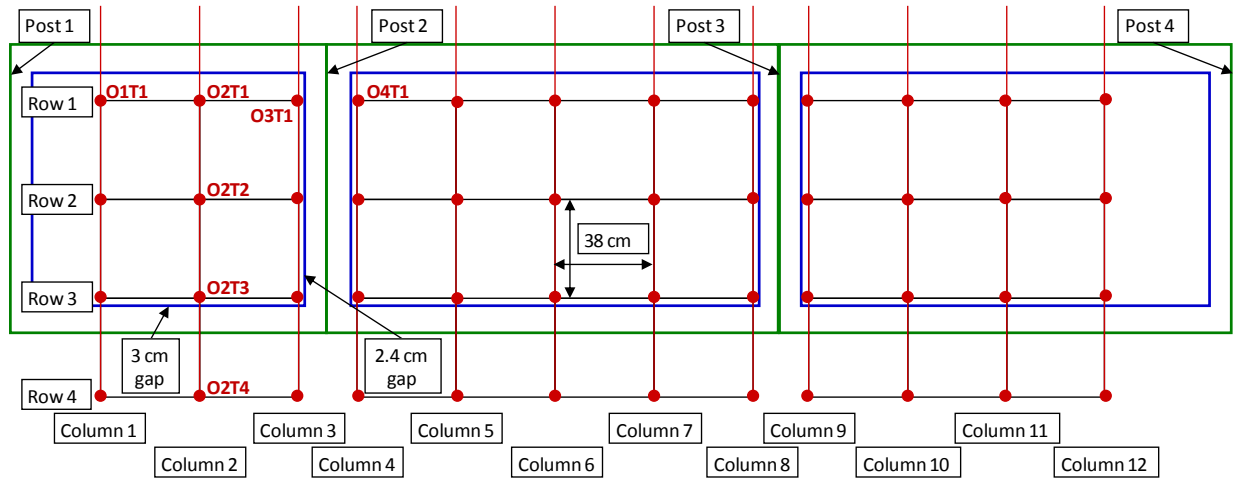


Figure 7 A schematic (top) and photograph (bottom) of the exterior grid of thermocouples on the motorcoach windows. The blue rectangles represent window outlines, red dots represent TCs, green areas represent window frames and post centerlines. Labels pertain to designations in the data file. The pattern of thermocouple labeling is shown in red with O for outside grid, the 1st number for column, and the 2nd number for row.

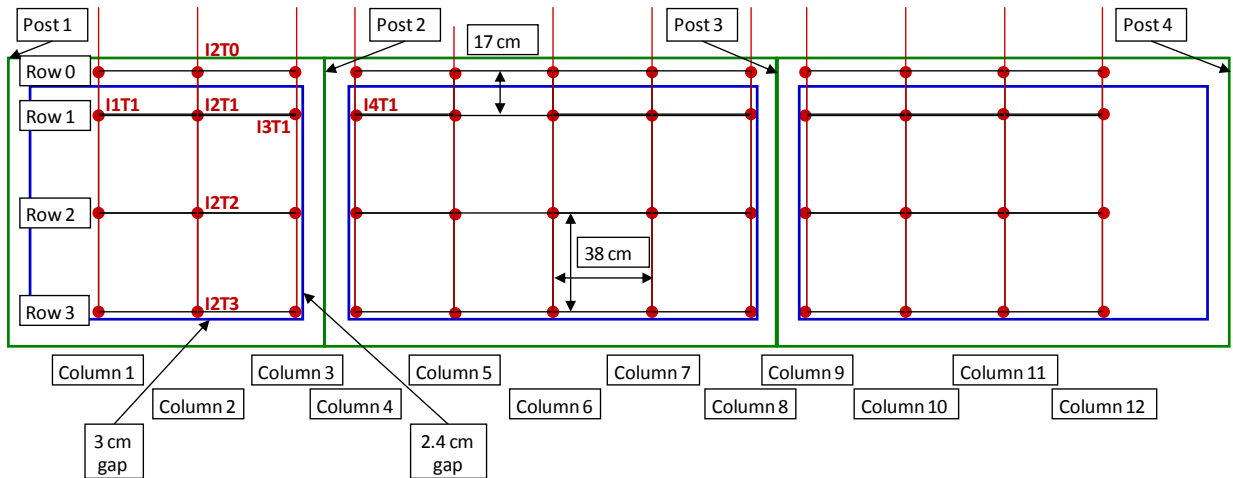
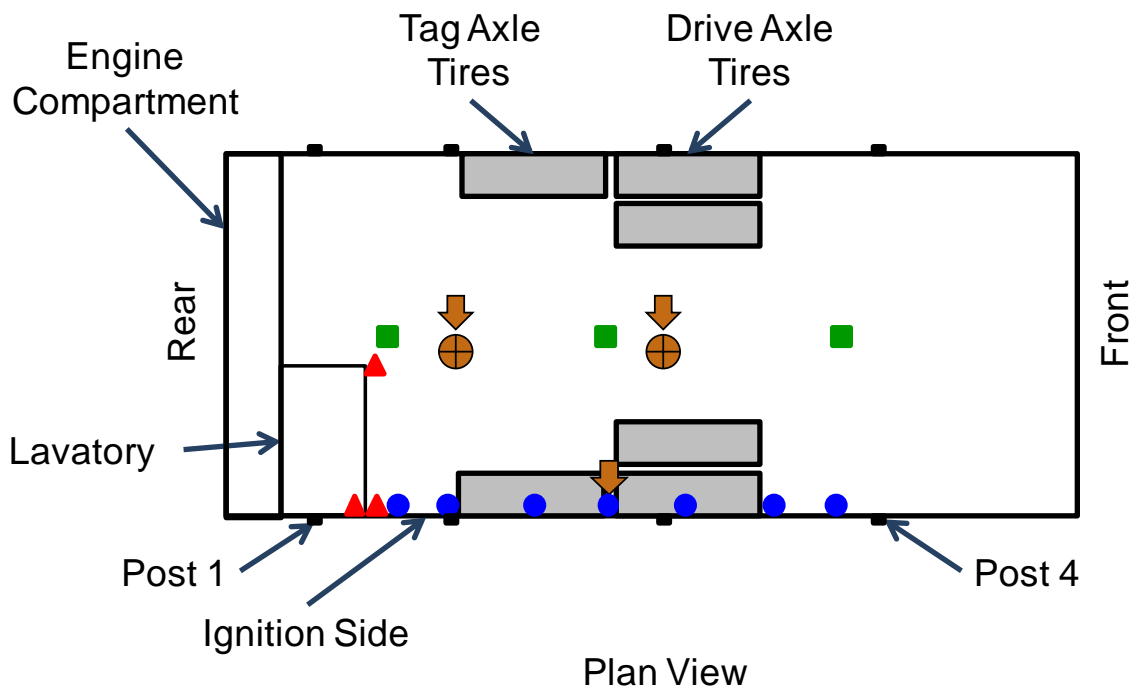


Figure 8 A schematic of the interior grid of thermocouples located near the windows. The blue rectangles represent window outlines, red dots represent TCs, green areas represent window frames and post centerlines. Labels pertain to designations in the data file. The pattern of thermocouple labeling is shown in red with I for inside grid, the 1st number for column, and the 2nd number for row.



- Heat Flux Gauges (5)
- Wall/Floor Thermocouples (7)
- Lavatory/Floor Thermocouples (3)
- Central Tunnel/Floor Thermocouples (3)

Figure 9 A diagram of the top view of the motorcoach showing approximate locations of interior floor thermocouples and the locations and directions of heat flux gauges.

Heat Flux

Heat flux was measured in 5 locations to help indicate the transfer of heat from the fire through the windows or floor. These measurements also provided insight as to when interior heat fluxes would have threatened to ignite materials if they had been present. Table 2 lists the locations and directions of the gauges, and Figure 9 is a diagram depicting the top view of the motorcoach and the approximate locations and directions of the gauges. Expanded uncertainties for the heat flux location measurements are estimated to be ± 2 mm. Figure 10 and Figure 11 are photographs of the installation of the gauges, and Figure 12 is a photograph of the gauge at the seat headrest location showing its proximity to the window. The heat flux gauges were water-cooled, Schmidt-Boelter type, which measured total heat flux, including both radiation and convection. The uncertainties (combined, expanded, relative) associated with the heat flux measurements were approximately ± 3 % based on the assumption that the measurement conditions were not significantly different from the gauge calibration conditions. [9]

Table 2 Heat flux gauge locations

Gauge Label	Location Description	Location Details
HFRS	Rear position, facing horizontally toward windows	127.8 cm from floor, centerline of bus, centered over rear tire (tag axle)
HFFS	Front position, facing horizontally toward windows	130.9 cm from floor, centerline of bus, centered over front tire.
HFRD	Rear position, facing down toward floor	132.8 cm from floor, centerline of bus, centered over rear tire (tag axle)
HFFD	Front position, facing down toward floor	133.8 cm from floor, centerline of bus, centered over front tire.
HFS _{Seat}	At seat headrest position, facing horizontally toward windows	111.2 cm from floor, 14.9 cm from window, centered between tires which is 51.8 cm rearward of rear facing side of window post 3 above front (drive axle) tire.

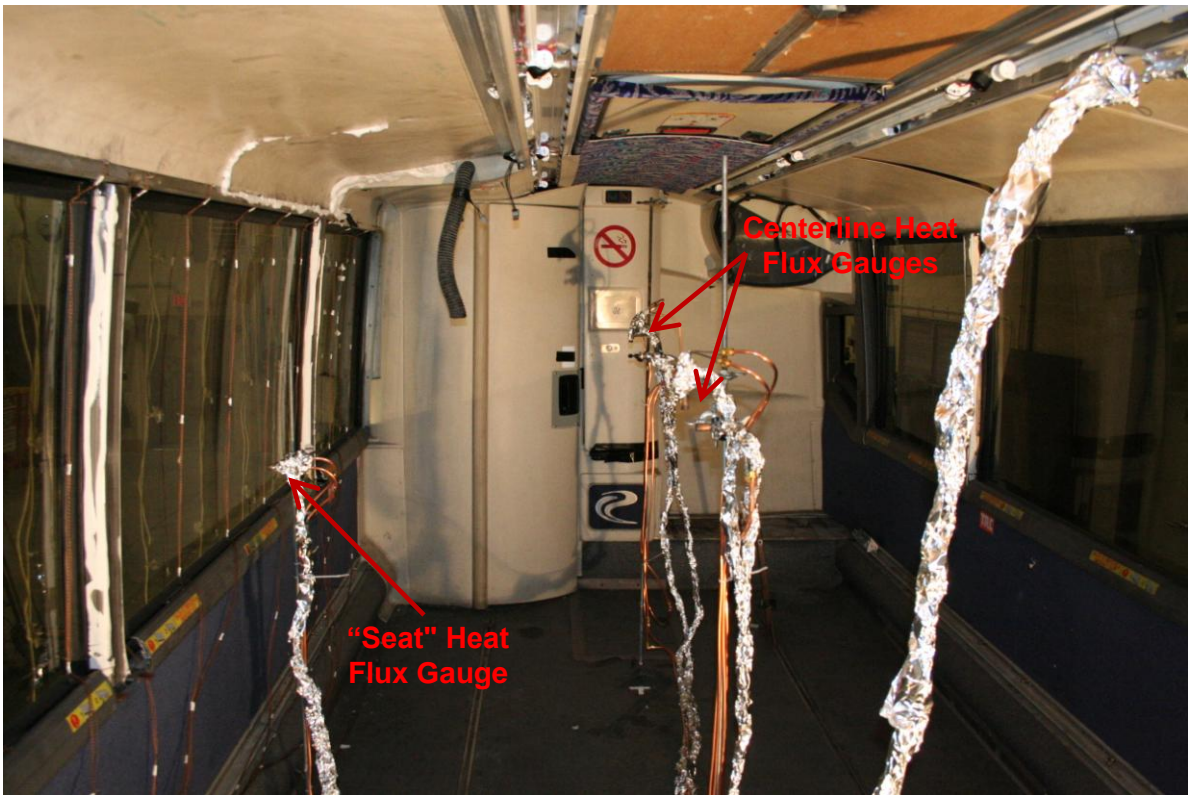


Figure 10 A photograph of the interior of the motorcoach showing the locations of the heat flux gauges.

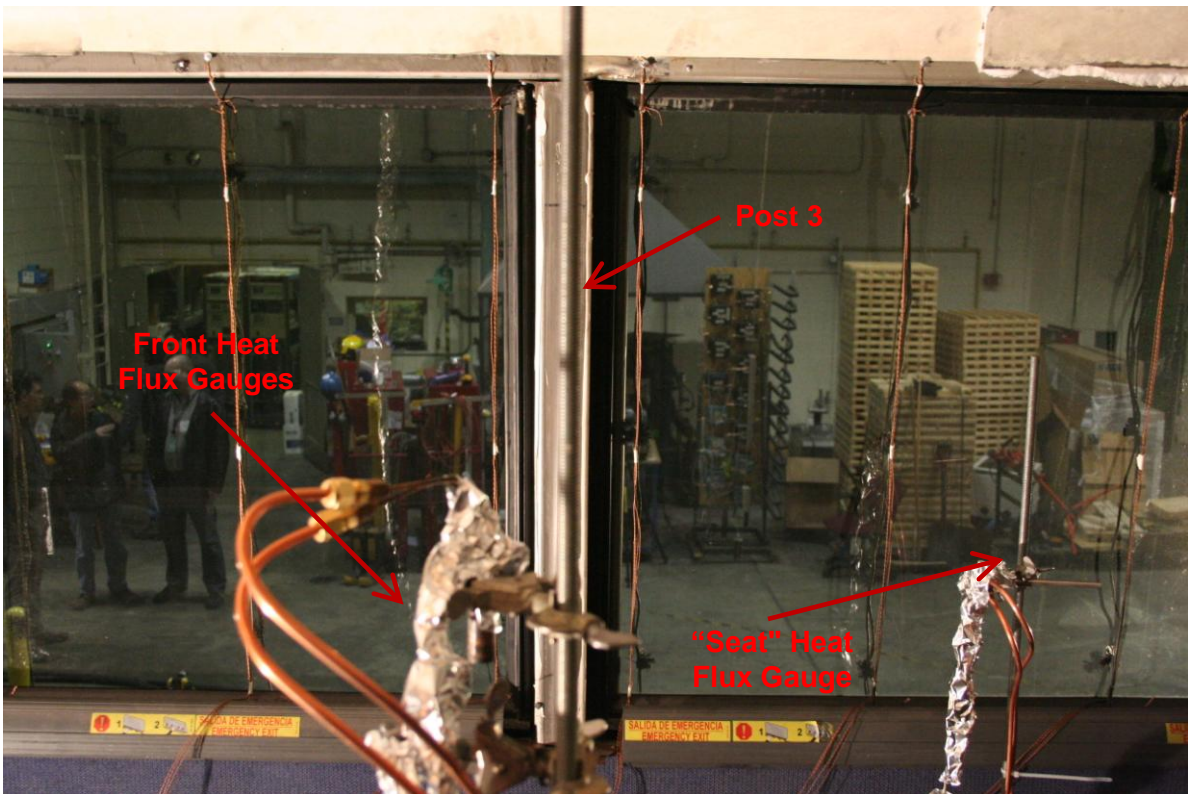


Figure 11 A photograph of the interior heat flux gauges and their view of the passenger side windows.

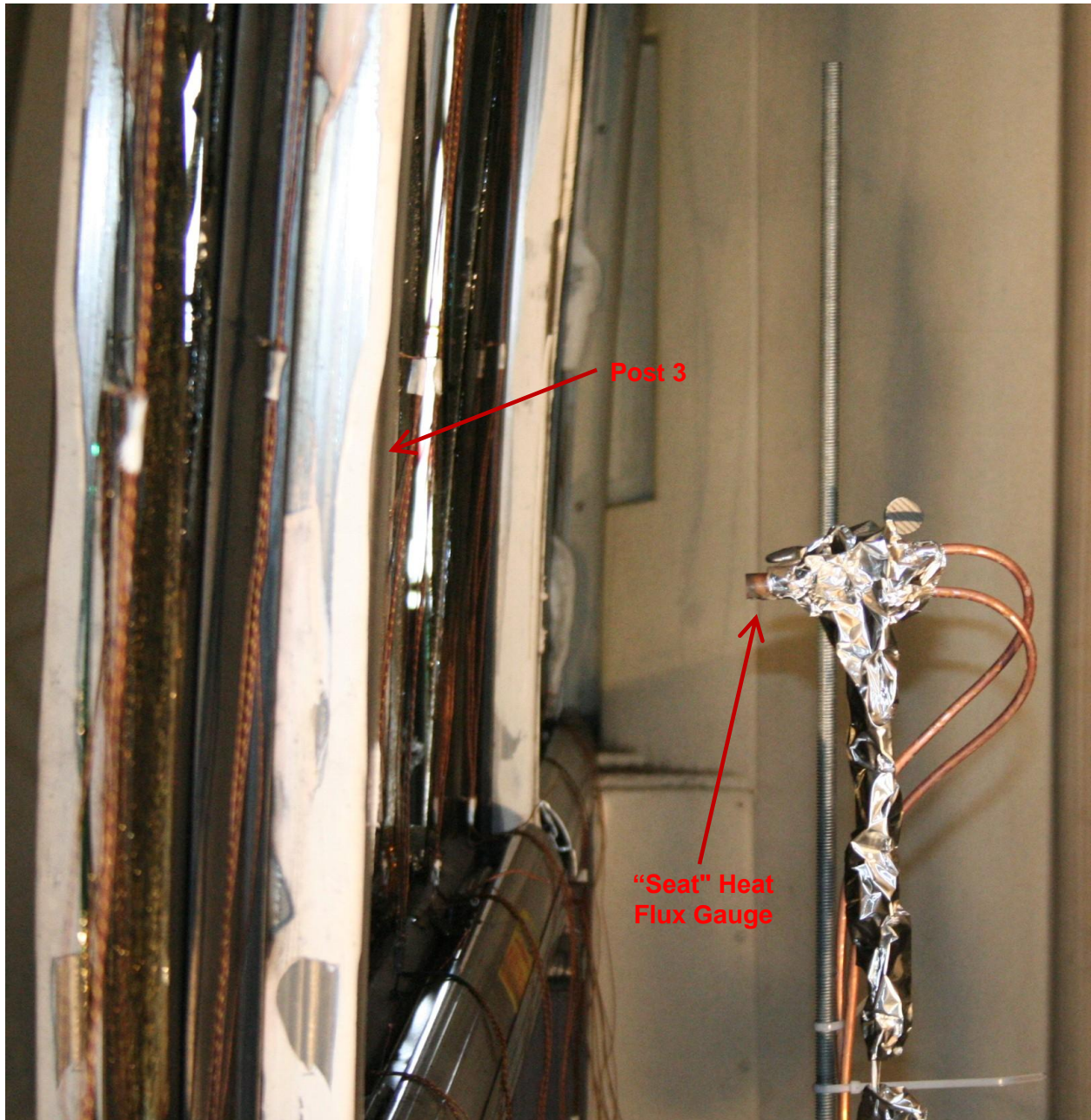


Figure 12 A photograph of the interior of the motorcoach showing the proximity to the window of the heat flux gauge at the position of a seat head rest.

Image Recording

Standard and Infrared Video

Seven standard and two infrared (IR) video recordings were made around and inside the motorcoach. The IR cameras were used to see if penetration of the fire into the passenger compartment could be better observed using infrared imaging. The positions of all of the cameras are shown in Figure 13. Two of the standard video cameras were high resolution versions. One was located at a position facing the tire fire from the side of the motorcoach, and the other was directed at the interior from a position several meters in front of the motorcoach's cut end. The video camera facing the tire fire from the side was paired with an infrared (IR) camera. Two other IR video cameras were mounted together on a ladder at the front end and trained on the interior, but one of these IR cameras was set to normal mode to provide contrast to the IR images. The two IR cameras on the ladder are shown in Figure 14. The remaining four video cameras were located closer to the motorcoach. These cameras were "bullet" type, low cost cameras for which damage from the fire was allowable. Figure 15 is a photograph of one of the bullet cameras in position on the far side (driver's side or left side facing forward) of the motorcoach between the axles. Figure 16 is a photograph of the bullet camera inside the passenger compartment opening, viewing the rear of the motorcoach interior. Interior lighting was added to improve image quality.

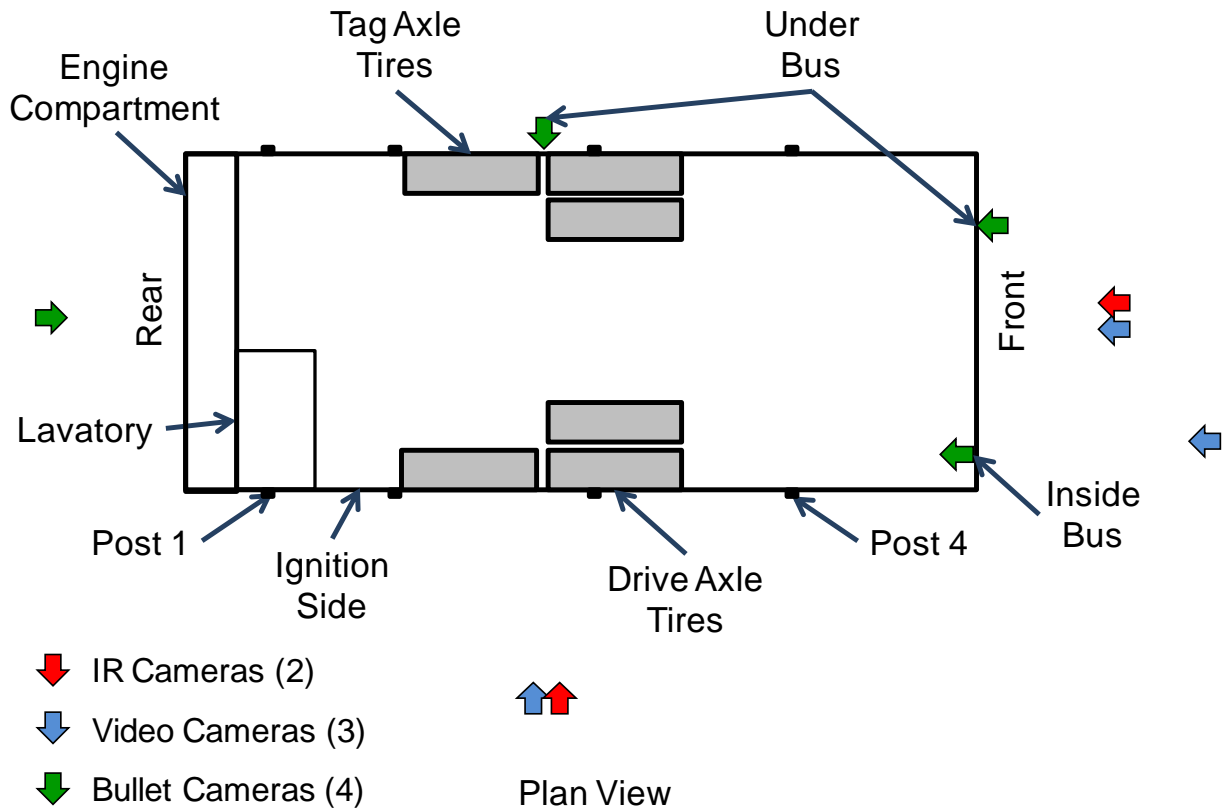


Figure 13 A diagram of the video camera layout showing their general locations and the directions they faced.



Figure 14 Photograph of the two IR cameras aimed at the open end of the motorcoach. One camera was set to IR and the other to visual mode for a head-to-head comparison.



Figure 15 A photograph of the bullet camera located between the two left (driver's) side axles.



Figure 16 A photograph showing the location of the passenger compartment bullet camera (lower left) and lighting (lower right) to provide better videos and photographs of the interior.

Still Photography

One main camera was used to take still digital photographs before, during, and after each experiment. Since the main camera was primarily located where it could view the passenger compartment from the open end and record fire penetration, it was supplemented during the second experiment with another digital camera, which captured more views of the developing fire involving the tire, wheel well, and exterior panel.

General Procedures

The following experimental procedure was followed on the day of each test:

- Conduct safety briefing for all personnel present in the building during experiments.
- Those personnel involved in igniting the burner and extinguishment put on turnout gear and self-contained breathing apparatus (SCBA).
- Initiate data collection and start recording with the standard and IR video cameras viewing the fire side of the motorcoach.
- Ignite the burner pilot (a long tube connected to a propane torch) with a lighter (butane).
- With the pilot located at the burner, open the gas valve, set the initial target HRR fuel flow, and adjust the air flow for pre-mixed, blue, conical flames.

- Place the natural gas burner adjacent to the wheel rim with flames impinging on the wheel.
- A few minutes before tire ignition, change tapes for the video cameras already running and start recording with all others.
- Cycle the halogen lights illuminating the motorcoach off and on to provide a synchronizing event for the video recordings.
- Heat the wheel until the tire is fully ignited (sustained flames on tire at bottom of the tag axle wheel or sustained flames between the drive axle tires). Target range for the pre-ignition heating period was 25 min to 40 min. The burner was maintained beyond intermittent ignition to ensure that the tire fire would progress and not self-extinguish.
- Close the natural gas valve and air valve and remove the burner.
- Determine whether fire has penetrated into the interior compartment through observation of the interior side of the flame impinged windows.
- Extinguish fire using a manned fire hose with water and foam (multiple hoses if necessary) once fire penetration into the interior compartment is determined. The fire was also to be extinguished and the experiment aborted if the fire HRR exceeded 6 MW or if significant smoke was observed escaping the exhaust hood and entering the high bay.
- Terminate data collection after recording several minutes of post-extinguishment measurements.
- Commence clean-up operations after surface temperatures have decreased to below 50 °C, smoke has sufficiently cleared the test bay and CO concentrations are less than 50 µL/L in the motorcoach (determined by the fire test Safety Officer).

RESULTS AND DISCUSSION

Event Timing

Both experiments initiated on each axle showed penetration of the fire into the passenger compartment through the long window between the axles. Table 3 lists the times and corresponding events for each experiment. The time referenced is when the burner was applied to the wheel. The uncertainty (combined, expanded) in the times listed is approximately ± 3 s. Table 4 lists the duration of the main periods of interest in these experiments: the period of heating before the tire was burning steadily, and the period between heating and penetration of the fire into the passenger compartment.

Sustained or established burning for the tag axle wheel fire was defined as continuous (versus intermittent) burning of the tire rubber at one or more locations in the bottom half of the tire (away from the top which received additional heat from buoyant convection). Sustained burning for the drive axle wheel fire was more difficult to determine since the flames were between the dual tires and mostly obscured. A consistent, non-intermittent flame plume proceeding from between the tires was considered sustained or sufficiently established burning for that experiment.

The periods of heating before sustained burning were quite different for each experiment with the experiment initiated on the tag axle wheel requiring about fifteen more minutes than the one initiated on the drive axle wheel. The likely reason for this is that the tag axle wheel had more conduits for heat loss than the drive axle wheel. The outside of the tag axle wheel was convex and exposed to ambient air, while the outside of the drive axle wheel was concave and recessed (see Figure 5). This allowed the drive axle wheel to trap more heat than the tag axle wheel. The heat from the burner that did not go into the tag axle wheel would be convected along the bottom of the shield and away, but for the drive axle wheel would heat the upper portion of the wheel first before reaching the shield. Also, while the back of the tag axle wheel could radiate and convect heat away, the drive axle wheel was connected to the second inner wheel, promoting overall heating of the dual tire system and blocking convective cooling on the backside of the outer wheel and tire. The rubber of the tires acts as an insulator as well, trapping heat between the tires and near their surfaces.

The period between heating and compartment penetration was about 1.5 min shorter for the tag axle experiment than for the drive axle experiment. While the time periods are both short and their difference could be due to random variation, there are some factors that could explain the distinction. The tag axle tire started burning on the outside and had access to air for more complete and hotter combustion. The drive axle tires started burning at the surfaces between the inner and outer tire, away from the outer surface of the outer tire. The narrow region between tires limited the flow of air and decreased the rate of growth. Also, the fire between the drive axle tires had to grow sufficiently to send a plume horizontally to spread outward and then upward onto the GRP fender and exterior panel. This extra path for fire spread took longer (363 s) than for the more direct path of the tag axle (280 s) up to the fender and panel.

Penetration was defined as fire entering the motorcoach by some path such as a hole created by the fire or evidence of flame spread into the interior due to the tire fire. In these experiments, both tire fires resulted in compartment penetration by breaking through the windows. If the floor had been the pathway of fire spread, observation of a sustained and growing fire in a region of the floor heated by the tire fire would have been required, but not necessarily a hole in the floor as occurred with the windows.

While breaking the windows was the path by which the fire penetrated into the passenger compartment, the windows did not break easily. The window design was two glass layers with a clear laminate layer between them. The inner glass was a safety type which shattered, and the outer was not. It is noteworthy that the glazing layers often broke independently from each other with the fire impinging on the outside. For the drive axle experiment, glass layers would sometimes fall in or out, but it took about 2 min from cracking of glass to the time that layers started falling away and another minute for any areas to have both layers break off, creating a hole and path for fire entry. Some of the pieces of glass with burning laminate fell inside and burned on the floor, but this was not considered fire penetration although it is possible that the burning material could have ignited seat cushions if they had been installed. Also, material between the front most window and post 3 was burning during the second test but was not considered fire penetration.

Table 3 Timing of events and observations during each experiment. (uncertainty = ± 3 s)

Test 1 (Heated Tag Axle Wheel)		Test 2 (Heated Drive Axle Wheel)	
Time (s)	Event Description	Time (s)	Event Description
-807	Data recording initiated	-1636	Data recording initiated
-53	Burner ignited	-26	Burner Ignited
0	Burner applied to wheel	0	Burner applied to wheel
189	Pool fire	452	Flare up (interesting)
1014	Flare up	609	Cameras started
1188	Starting cameras	695	Last camera activated
1361	Flare up	722	Flashed lights for camera sync
1382	Flashed lights for camera sync	760	Smoke from back of tire
1860	Intermittent ignition	789	Smoke on backside of bus
1918	Intermittent ignition at tire bottom	979	Smoke coming from inside wheel at the 12 o'clock (top) position
1972	Steady ignition at top of tire	1185	Ignition in the back of outside tire
2170	Fender ignited	1255	Gas off
2177	Burner removed	1278	Flames licking at outside molding
2390	Smoke inside at bottom of tree 6	1355	Melt dripping of fender plastic
2457	Window penetration, suppression start	1417	Glass cracking, flaming inside
2469	Extinguishment	1504	Flames along inside post 3
		1582	Panes of glass breaking
		1603	Sustained flames on inside
		1618	Window penetration, suppression start
		1632	Suppression complete
		1712	Exhaust flow increasing

Table 4 Duration of periods of heating and between heating and penetration.

Period	Duration (s)	
	Test 1 (Heated Tag Axle Wheel)	Test 2 (Heated Drive Axle Wheel)
Burner heating wheel to steady tire burning	2177	1255
Burner stopped to fire penetration of passenger compartment	280	363

Heat Release Rate

For the first test, the average LFL exhaust hood flow was 19.2 m³/s (40 600 ft³/min). A setting was selected close to the maximum flow for one of two exhaust trains since the potential size of the tire/motorcoach fire was unknown. Since the hood flow proved more than adequate for the first test, the setting was maintained for the second, and the average flow was 20.1 m³/s (42500 ft³/min). The peak heat release rates were 1162 kW and 1465 kW for the first and second tests, respectively. Figure 17 and Figure 18 show the HRRs plotted versus time for the two experiments. The time of passenger compartment penetration is marked with a vertical line. Suppression was initiated within 5 s of penetration and is indicated by the sudden drop in HRR.

The uncertainty of the HRR measurement for the period immediately preceding each peak was ±9.1 %. The peak values were also attenuated by about 1 % due to the time response of the calorimetry system to transients. [6] Taking this into account, the revised values for the two tests were 1175 kW ± 107 kW and 1480 kW ± 135 kW, respectively. The rates of increase of each fire were between 300 kW/min and 400 kW/min during the final 2 min of each test.

The natural gas burner HRR was calculated using measurements of the gas flow, temperature, and pressure and a chemical analysis of the natural gas. The calculated average values were 61.7 kW for the first test and 60.3 kW for the second. These values each have uncertainties of about ±2.5 %. [6]

For the first test, the total heat released by the burner and motorcoach materials was 323 MJ, which consisted of 138 MJ (43 %) from the burner and 185 MJ (57 %) from the bus materials. For the second test, the total heat released by the burner and motorcoach materials was 341 MJ, which consisted of 77 MJ (32 %) from the burner and 264 MJ (77 %) from the bus materials. The total heat released during each test was similar, but the drive axle test required much less heating (56 %) for the reasons described in the previous section on event timing. During the drive axle test (#2), 43 % more bus material was burned than in the tag axle test (#1). The drive axle tire fire actually spread to the tag axle tire causing two plumes to merge and involving more of the exterior panel than the single plume from the tag axle test. Also, the tires and exterior panels burned longer before penetration during the drive axle test.

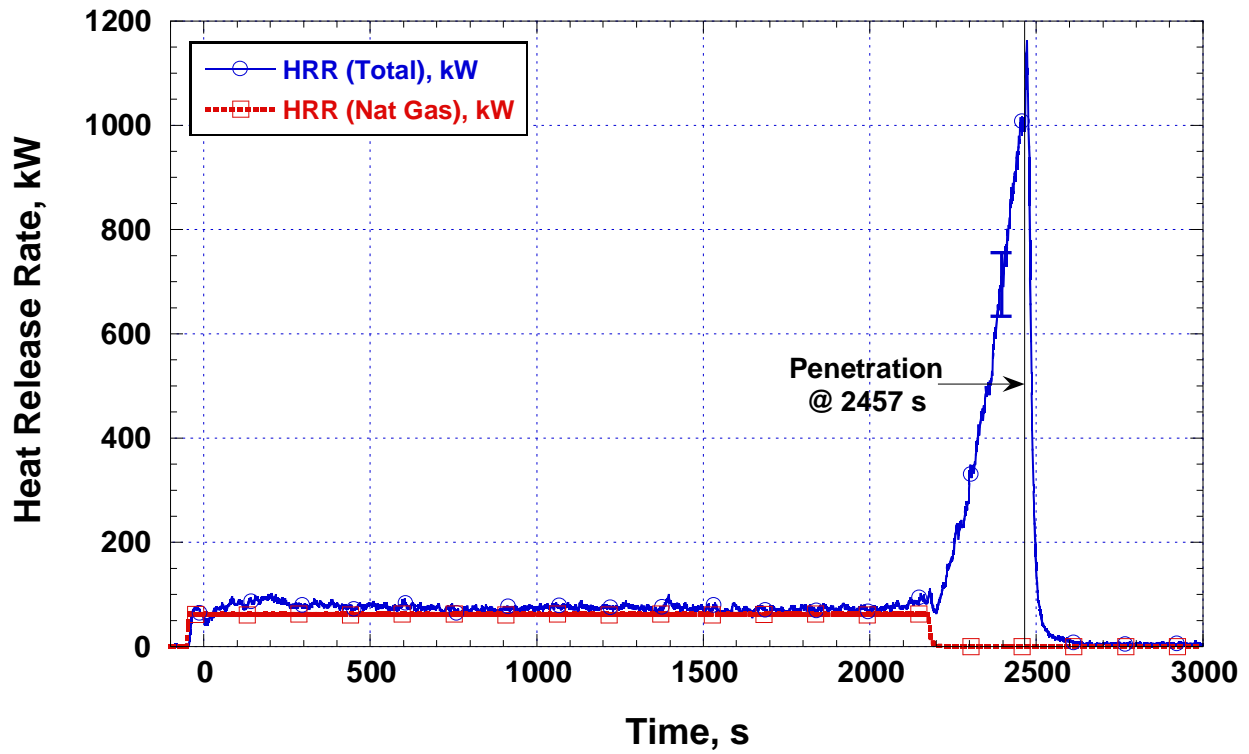


Figure 17 Heat release rate plotted versus time for test 1, the heated tag axle wheel experiment.

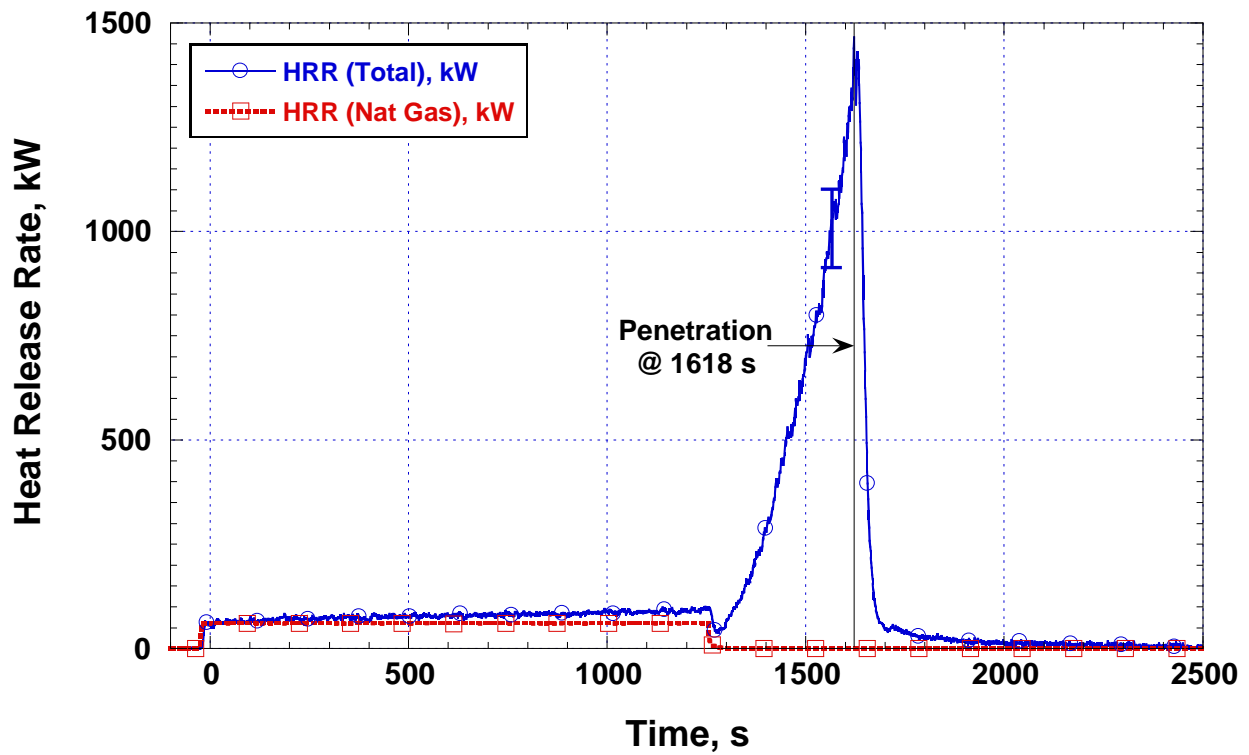


Figure 18 Heat release rate plotted versus time for test 2, the heated drive axle wheel experiment.

Wheel, Tire, and Wheel Well Temperatures

For thermocouples on surfaces exposed to heating by the burner, the measured temperatures have uncertainties of approximately ± 10 °C. For gas temperatures in this and following sections, consider for thermocouples impinged by fire that the temperatures recorded may have been as much as 10 % (90 °C) low for a 600 °C reading and 20 % (220 °C) low for an 850 °C reading.

Figure 19 and Figure 20 are plots of temperature versus time for the wheel and tire thermocouples on the passenger side of the motorcoach. Figure 6 shows the labeling scheme used in the plot legends, and Appendix B provides more detailed location descriptions for these and subsequent plots. For the heated tag axle wheel experiment, the wheel temperatures only led the tire temperatures by about 40 °C. According to Table 3, some intermittent ignition of the tire was occurring at 1860 s. By that point, the tire temperatures at the top and bottom positions had exceeded 360 °C. At that same time, the maximum wheel temperatures had just surpassed 400 °C. For the heated drive axle wheel experiment, the wheel temperatures led the tire temperatures by 100 °C to 150 °C. This is easily explained by the fact that the tire temperatures were measured on the outside interface between the tire and wheel rim, but wheel thermocouples were located on the inside surface of the wheel between the outer and inner wheels. Also, the heat from the burner was focused at the inside surface of the wheel which preferentially heated up the inside parts of the tire as well. At the time when flames were seen rising between the tires, the wheel temperatures all exceeded 420 °C. Because a lot of smoke was visible and some wheel temperatures exceeded 400 °C about 7 min prior to visible flames, it's likely that a smoldering or small flaming fire existed between the tires well before flames were seen.

Wheel well gas temperature plots are shown in Figure 21 and Figure 22. The heated tag axle wheel experiment produced the highest temperatures (850 °C) directly over the rear tire and the second highest temperatures (650 °C) directly behind and between the tag and drive axle tires. For the heated drive axle wheel experiment, all but the front most temperature exceeded (900 °C). Far (driver's) side wheel well temperatures were rising, but were below 300 °C at the time of penetration. For the minute prior to penetration, the far side wheel well temperatures were rising at about 20 °C/min for the tag axle test and between 40 °C/min and 60 °C/min for the drive axle test.

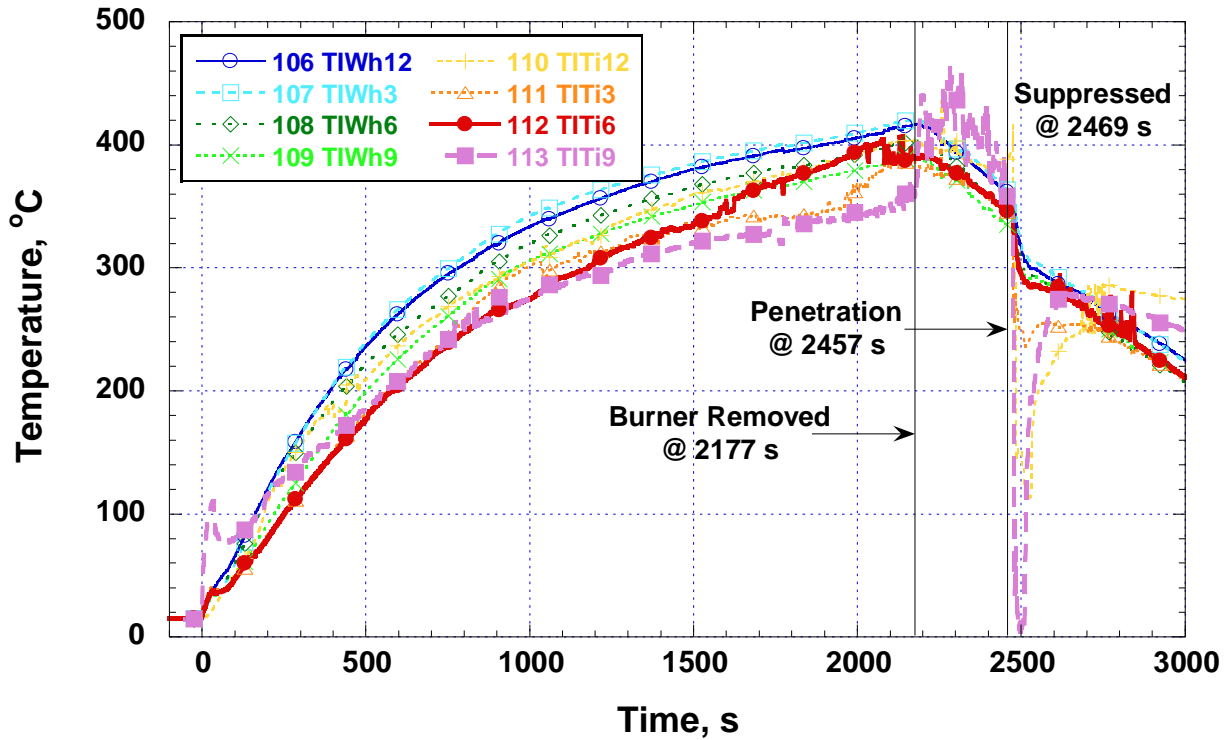


Figure 19 A plot of test 1 (tag axle) temperatures versus time for the heated wheel (Wh) and tire (Ti). Numbers in the labels represent 12, 3, 6, and 9 o'clock positions (0°, 90°, 180°, and 270° from top).

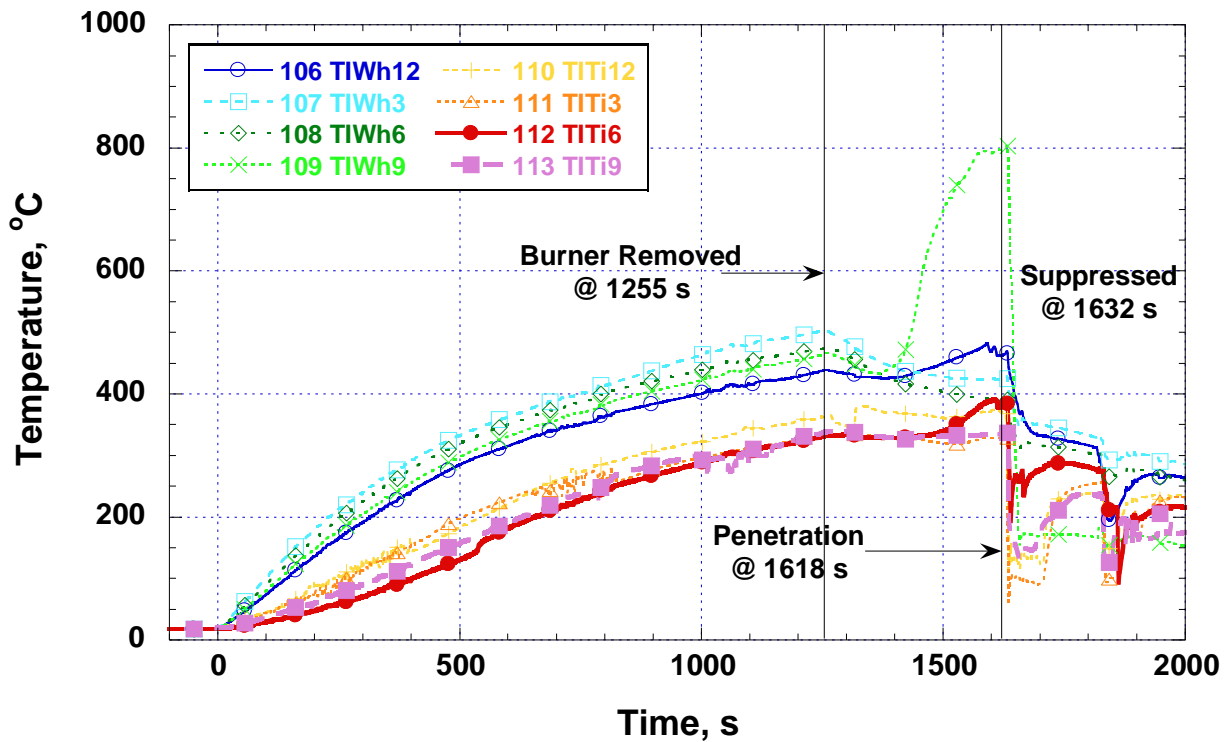


Figure 20 A plot of test 2 (drive axle) temperatures versus time for the heated wheel (Wh) and tire (Ti). Numbers in the labels represent 12, 3, 6, and 9 o'clock positions (0°, 90°, 180°, and 270° from top).

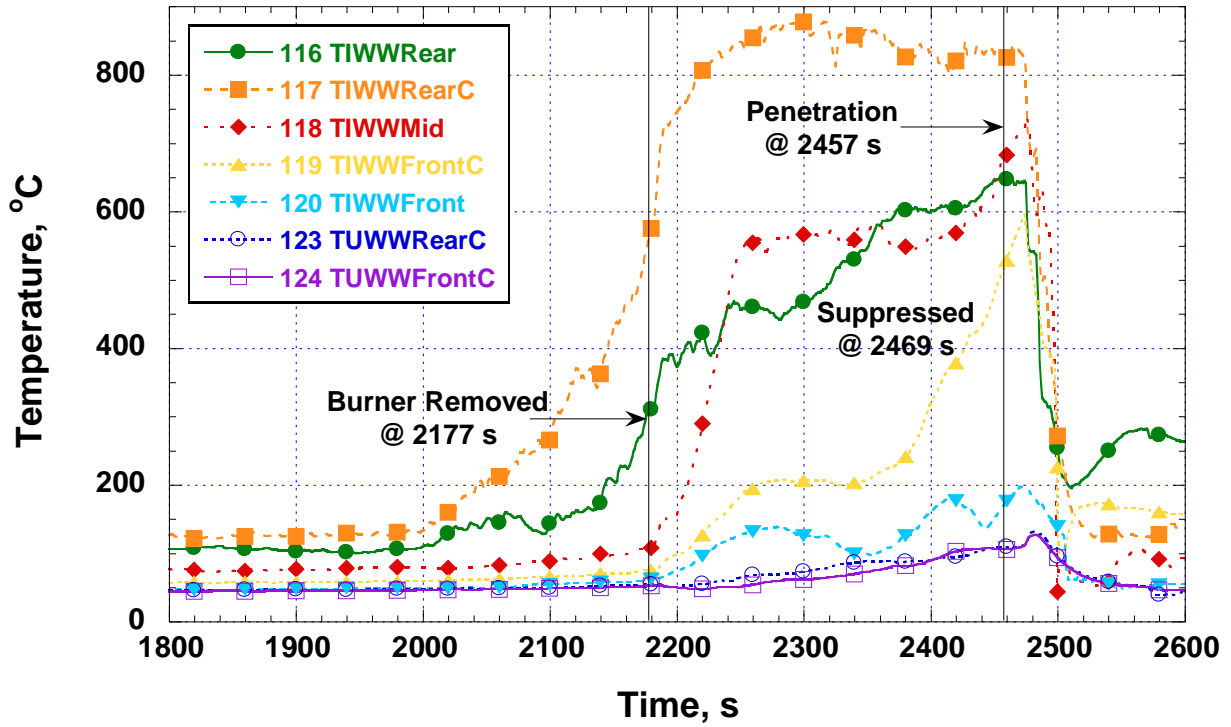


Figure 21 A plot of test 1 (tag axle) temperatures versus time for the wheel wells. I and U represent ignited and unignited sides, respectively.

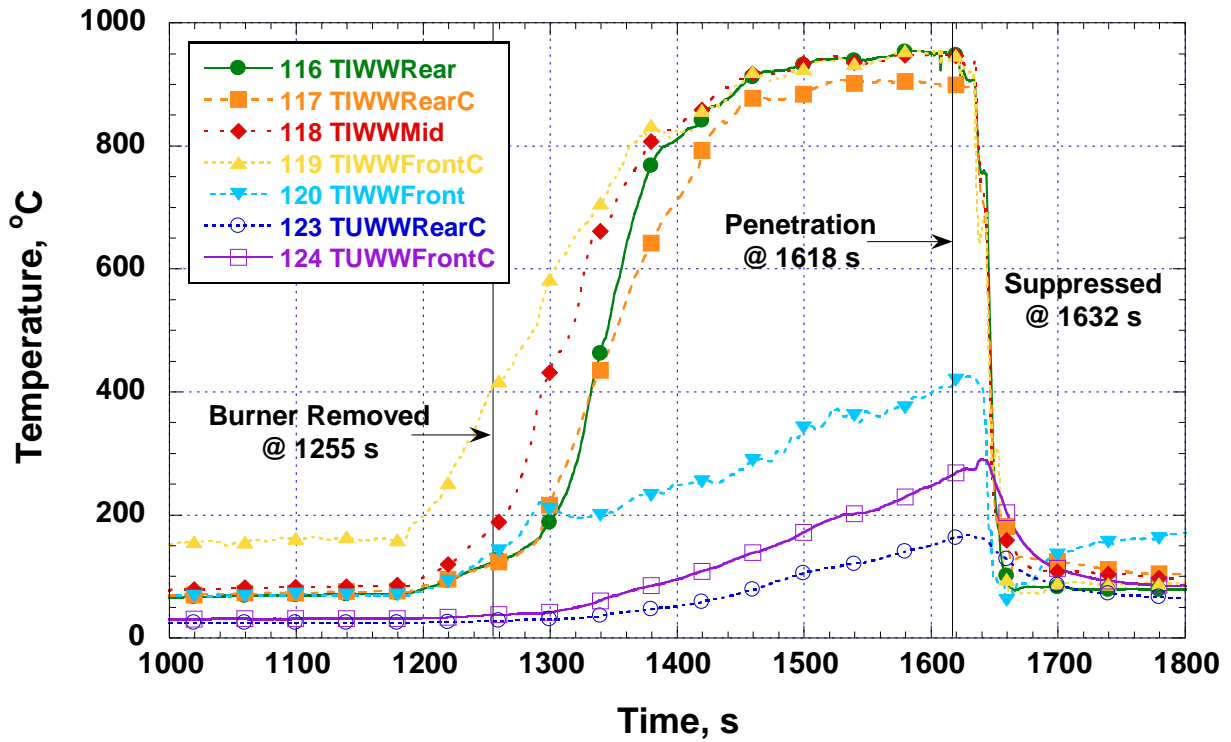


Figure 22 A plot of test 2 (drive axle) temperatures versus time for the wheel wells. I and U represent ignited and unignited sides, respectively.

Window and Panel Temperatures

Figure 23 and Figure 24 are plots from both experiments of temperature versus time for the exterior thermocouples located over the GRP paneling just below the window line. Refer to Figure 7 for familiarization with the exterior thermocouple locations and Figure 8 for the interior locations. The plots show that before penetration for both experiments, the temperatures in columns 5 to 9 were much higher than those for columns 1 to 4 and 10 to 12 with the exception of column 7 for test 2 which had a lower temperature. For both tests, the temperatures for columns 5 to 9 ranged from 600 °C to 850 °C except for test 2 column 7 which had a temperature of 400 °C at penetration. Column 7 is located just forward of the midpoint between the two axles so the separate fire plumes apparently did not impact the space between each other as severely as the space directly above.

Figure 25 and Figure 26 are plots from both experiments of temperature versus time for the highest exterior thermocouples located near the tops of the windows. For test 1, columns 5 to 9 are again the hottest. For test 2, columns 8 and 9 temperatures are high early with columns 5 and 6 (over the tag axle tire) lagging behind by about 1.5 min and 3 min, respectively. As with the lowest position on the panel, column 7's temperature lags even farther behind as it is in between the main plumes.

Figure 27 and Figure 28 are plots from both experiments of temperature versus time for the lowest interior thermocouples located about 3 cm from the bottom of the windows. For test 1, the column 6 thermocouple approached 200 °C for about 30 s and briefly exceeded 600 °C at penetration while the other interior temperatures remained below 100 °C. This indicates that the windows acted as fairly successful thermal barriers until actual penetration, which occurred near column 6. For test 2, column 8 rose steadily to 200 °C for the 3 min prior to penetration and then quickly exceed 500 °C along with the column 9 temperature. Again, except when breakthrough occurred, the temperatures remained relatively low.

Figure 29 and Figure 30 are plots from both experiments of temperature versus time for the hottest columns of interior TCs, column 6 and column 8 for test 1 and test 2, respectively. T3 is the lowest position and T0 is above the window. For test 1, column 6 temperature in position T3 rises from 60 °C to 200 °C in the 25 s prior to penetration. T1 and T2 rise from about 45 °C to about 70 °C in the 25 s prior to penetration. For test 2, column 8 temperatures except for position T0 rise from about 200 °C to about 400 °C in the 30 s before penetration. Both plots show a rapid degradation of the windows in the 30 s prior to penetration, when temperature changes inside the window accelerate dramatically.

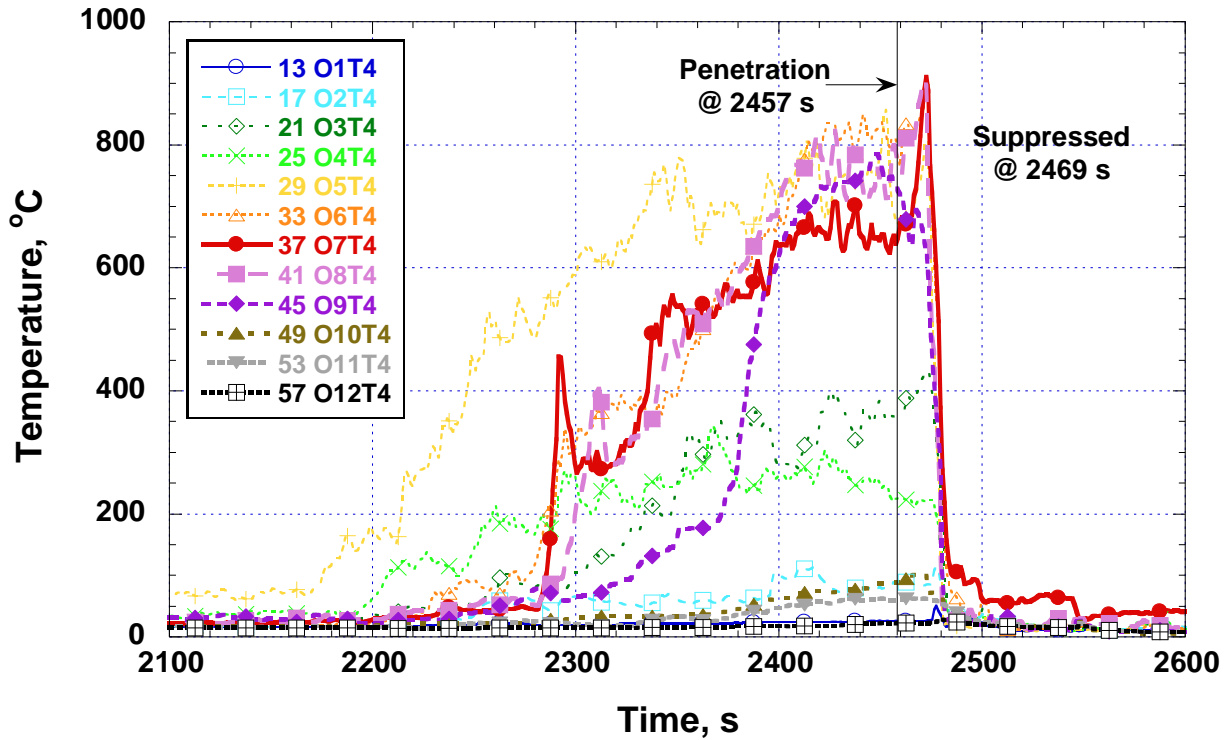


Figure 23 A plot of test 1 (tag axle) temperatures versus time for the lowest row of exterior TCs located below the window line 1 cm from the exterior GRP panel. See Figure 7 for labeling system.

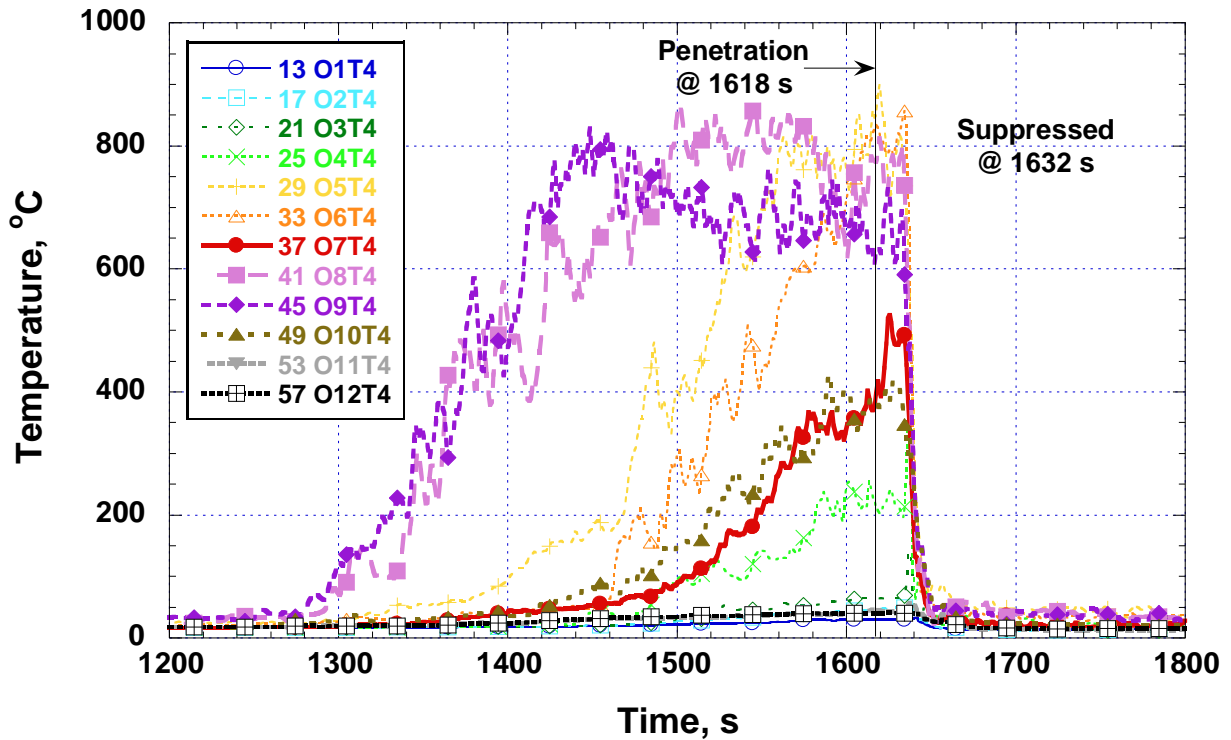


Figure 24 A plot of test 2 (drive axle) temperatures versus time for the lowest row of exterior TCs located below the window line 1 cm from the exterior GRP panel. See Figure 7 for labeling system.

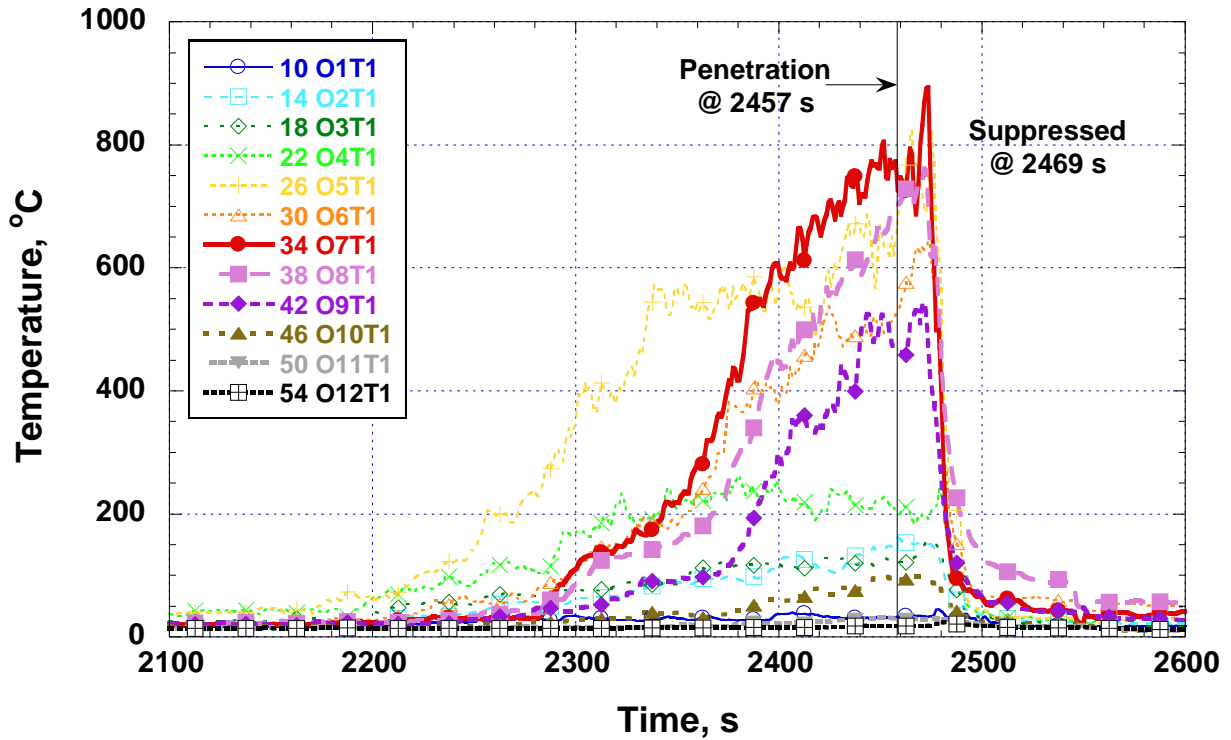


Figure 25 A plot of test 1 (tag axle) temperatures versus time for the highest row of exterior TCs located 1 cm from window surfaces and about 10 cm from the top of the windows. Figure 7 shows labeling.

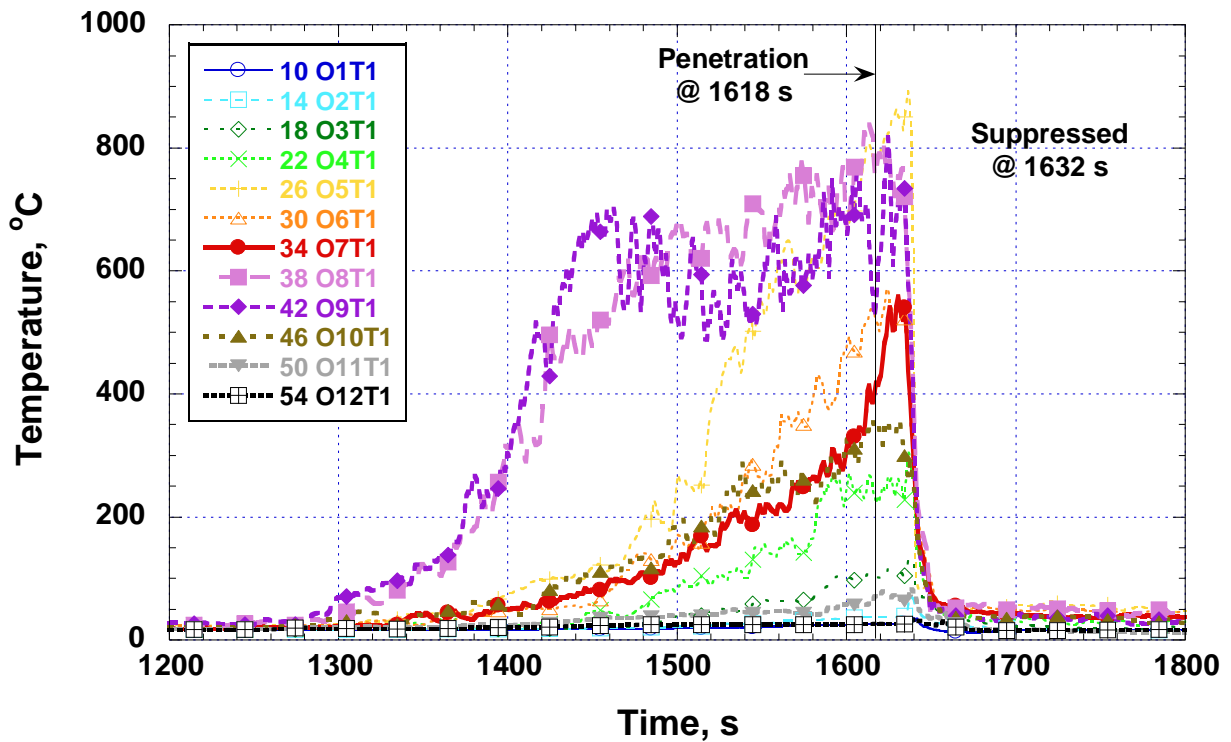


Figure 26 A plot of test 2 (drive axle) temperatures versus time for the highest row of exterior TCs located 1 cm from window surfaces and about 10 cm from the top of the windows. Figure 7 shows labeling.

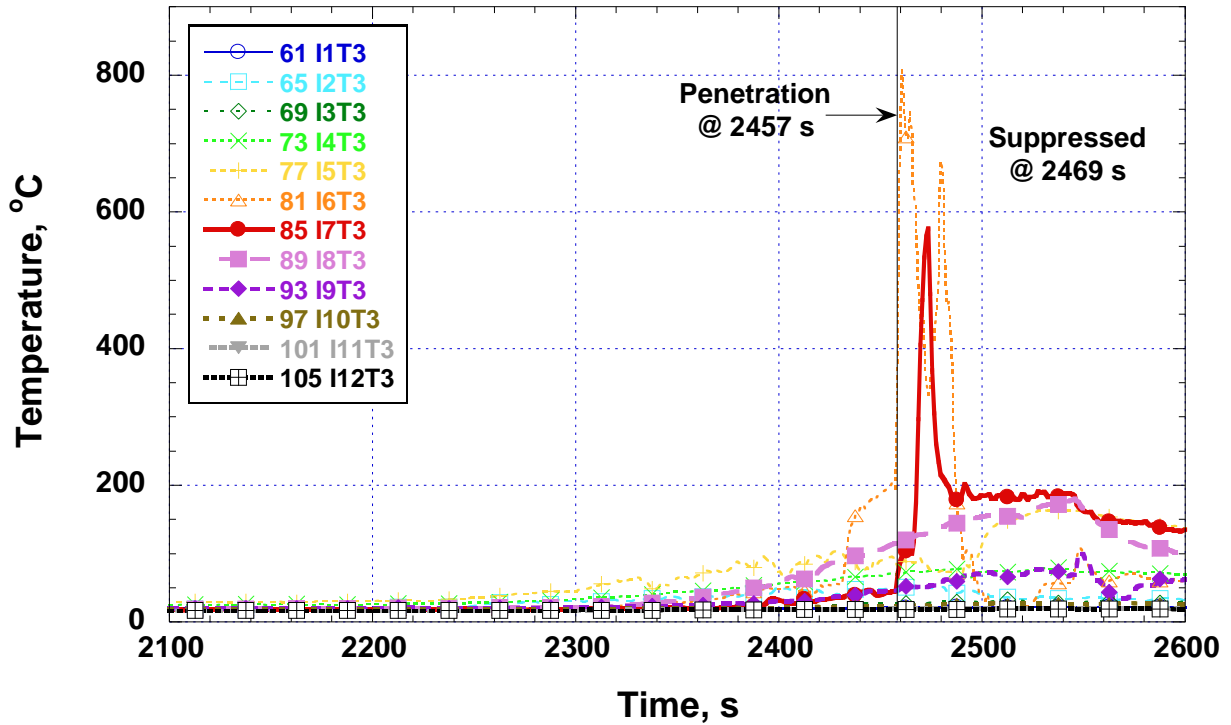


Figure 27 A plot of test 1 (tag axle) temperatures versus time for the lowest row of interior TCs, 1 cm from window surfaces and about 3 cm from the bottom of the windows. Figure 8 shows labeling.

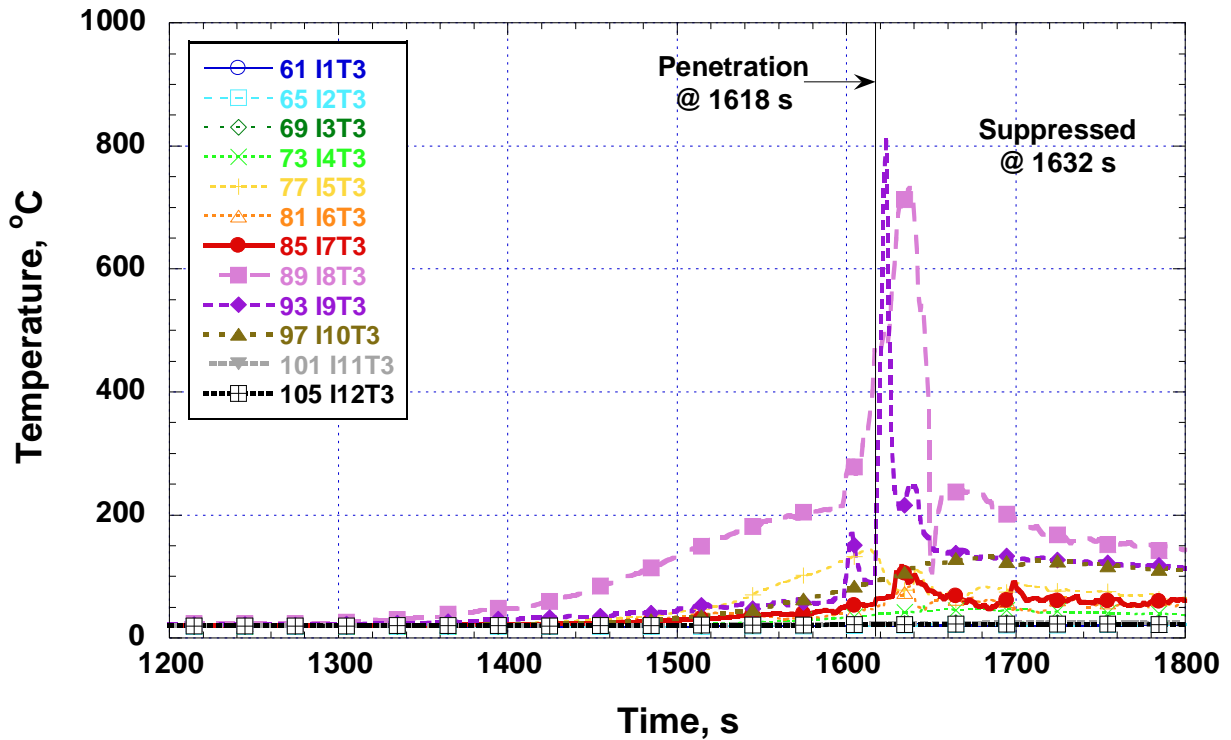


Figure 28 A plot of test 2 (drive axle) temperatures versus time for the lowest row of interior TCs, 1 cm from window surfaces and about 3 cm from the bottom of the windows. Figure 8 shows labeling.

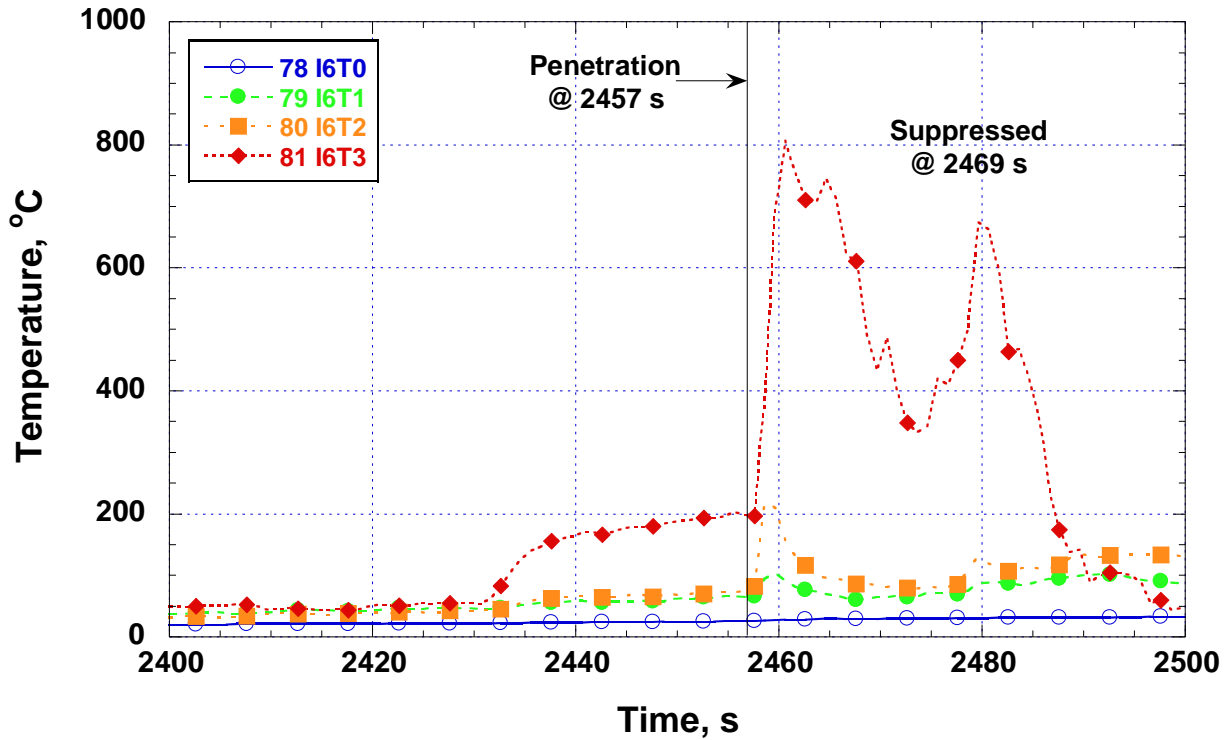


Figure 29 A plot of test 1 (tag axle) temperatures versus time for the hottest column of interior TCs, tree 6, 1 cm from window. T0 was located above the window. See Figure 8 for labeling system.

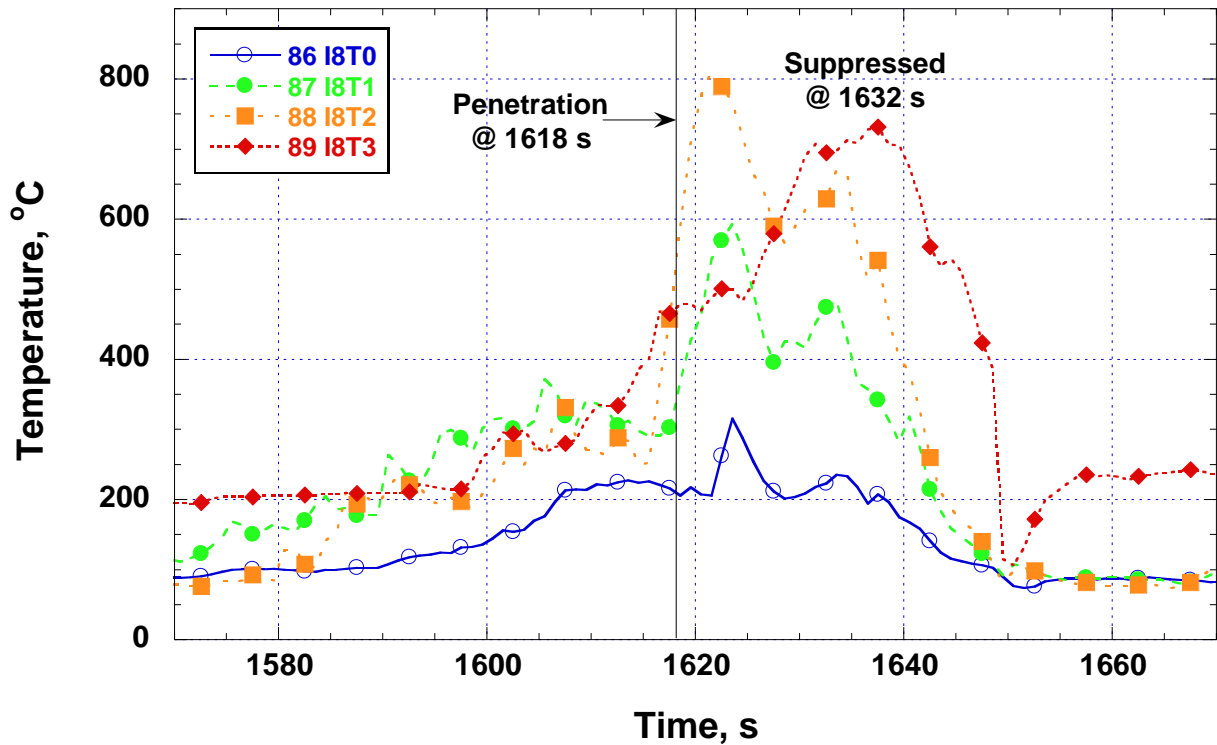


Figure 30 A plot of test 2 (drive axle) temperatures versus time for the hottest column of interior TCs, tree 8, 1 cm from window. T0 was located above the window. See Figure 8 for labeling system.

Floor, Lavatory, and Central Tunnel Temperatures

Floor, lavatory floor, and central tunnel temperatures were monitored because the path of the fire penetration into the passenger compartment was unknown and the floor was deemed to have a significant possibility of being that path. The central tunnel runs under the central aisle and contains tubing and wiring harnesses. Refer to Table 1 and Figure 9 to review locations of these measurements. Figure 31 and Figure 32 show the temperatures of thermocouples along the floor by the passenger side wall. All of the temperatures show barely any impact from the nearby fire and remain near the ambient starting temperatures. This revealed that the floor structure for this particular motorcoach was insulated from the tire fire's heat. Inspection of the floor design showed between 15 cm and 20 cm of fiberglass thermal insulation under the floor in the vicinity of the fire. Figure 32 does show a sharp rise just before test 2 penetration of the temperature midway between the tires, but it is only a rise of about 15 °C and may be related to some piece of glass with burning laminate attached or debris that fell from the window.

The lavatory floor temperatures shown in Figure 33 and Figure 34 only rose about 1 °C during each test. The floor area near the lavatory is similarly protected as the wall/floor areas from heating from below.

The central tunnel plots of temperature in Figure 35 and Figure 36 show some heating behavior. The test 1 front position rose 7 °C, but the change occurred after penetration and extinguishment. The test 2 front position rose over 25 °C prior to penetration and the center position rose about 15 °C after penetration. The small temperature increase for any of these positions indicates that the central tunnel under the center of the floor is protected sufficiently for this particular motorcoach to not be a likely pathway for passenger compartment penetration in the *early* stages of a tire fire.

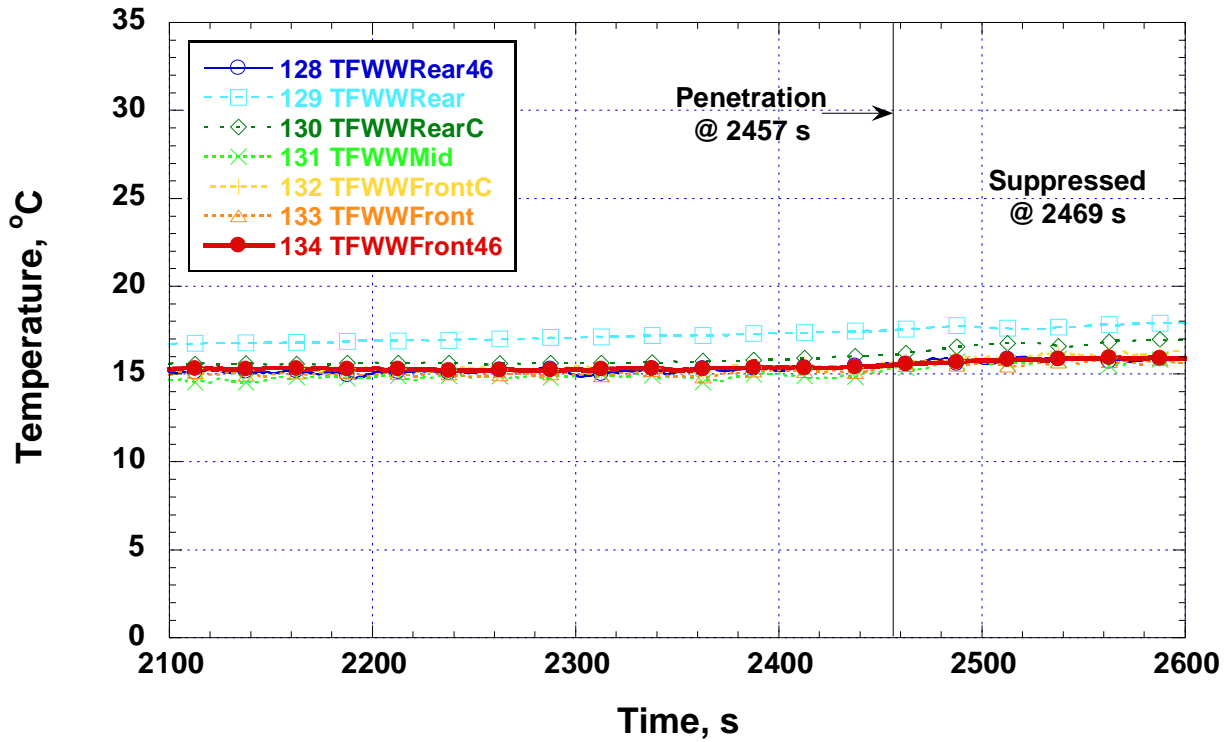


Figure 31 A plot of test 1 (tag axle) temperatures versus time for TCs on the interior floor at the bottom of the passenger side wall. Table 1 and Figure 9 describe thermocouple locations.

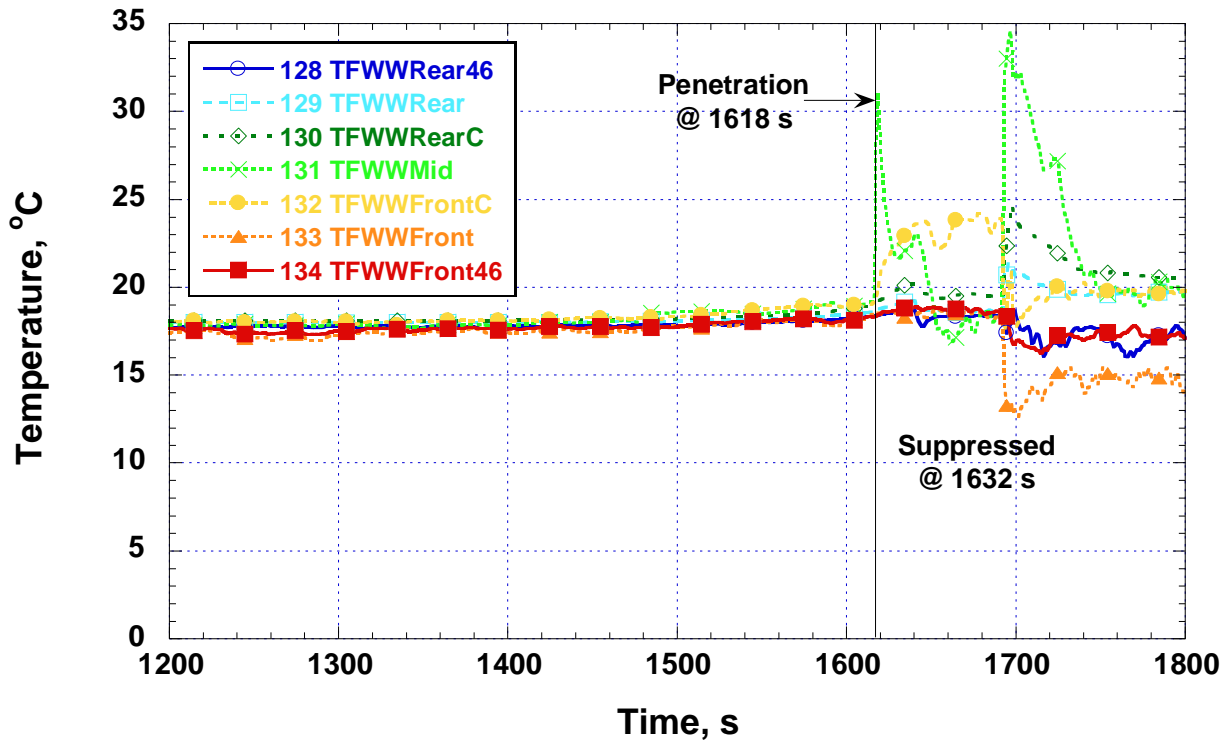


Figure 32 A plot of test 2 (drive axle) temperatures versus time for TCs on the interior floor at the bottom of the passenger side wall. Table 1 and Figure 9 describe thermocouple locations.

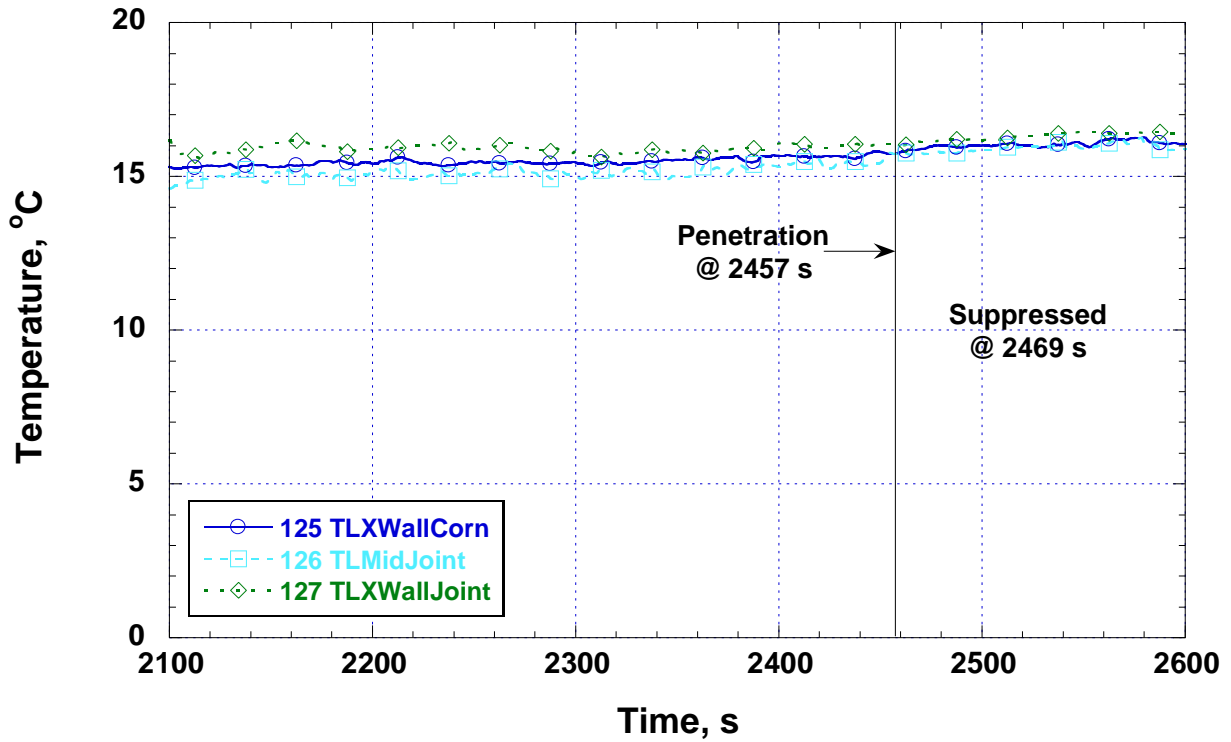


Figure 33 A plot of test 1 (tag axle) temperatures versus time for TCs on the interior floor where the lavatory walls join the exterior wall and floor in the middle of the coach. See Table 1 and Figure 9.

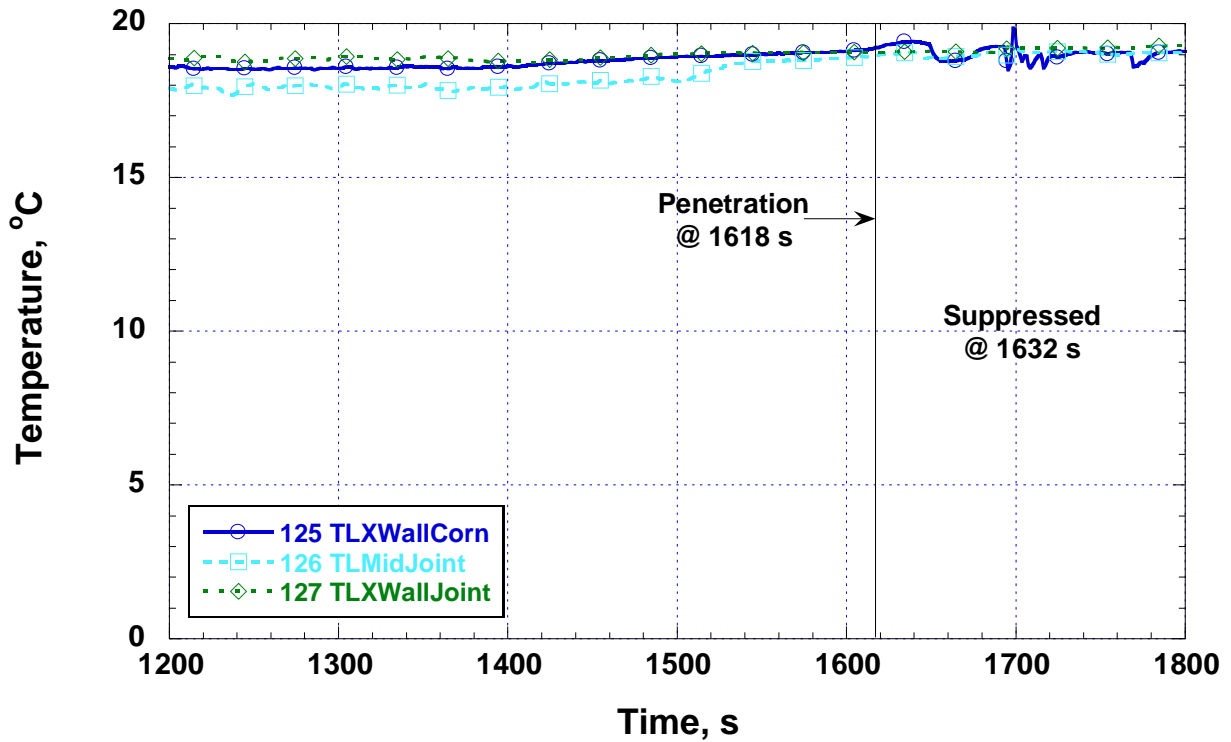


Figure 34 A plot of test 2 (drive axle) temperatures versus time for TCs on the interior floor where the lavatory walls join the exterior wall and floor in the middle of the coach. See Table 1 and Figure 9.

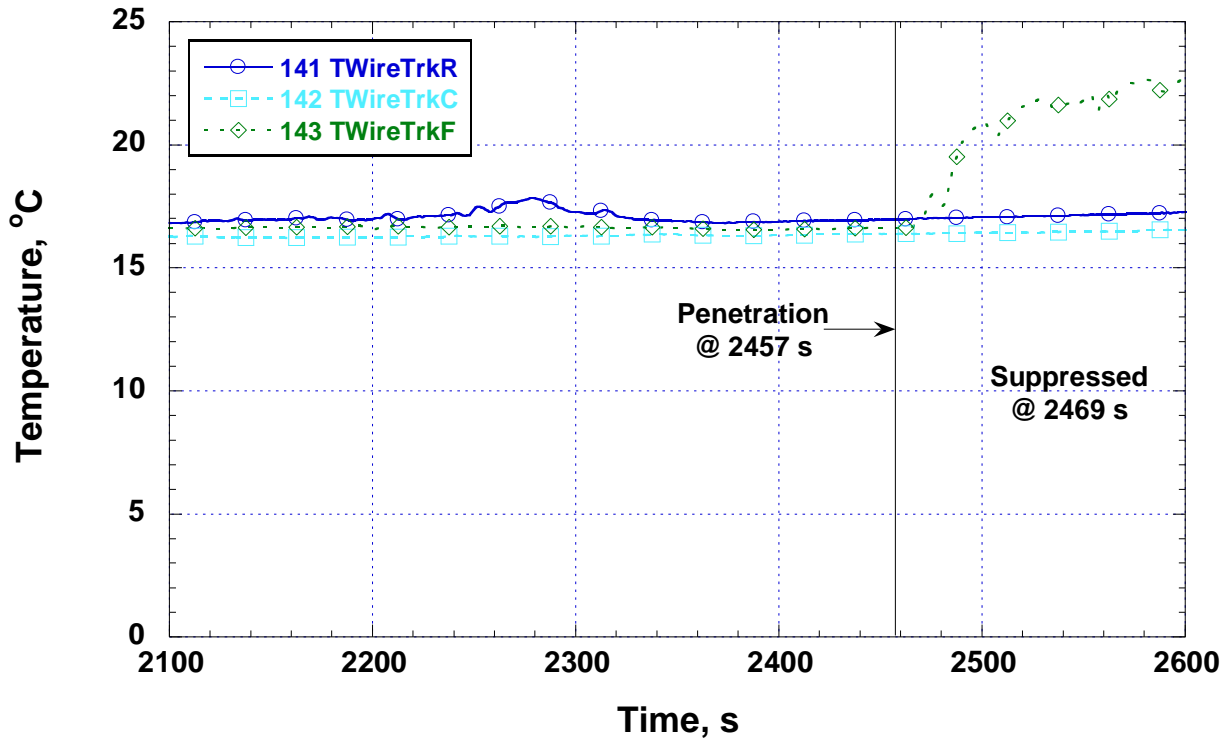


Figure 35 A plot of test 1 (tag axle) temperatures versus time for TCs inside the central tunnel for wires under the interior floor along the centerline of the coach. R, C, and F represent rear, center, and front, respectively, of the test section. Table 1 and Figure 9 describe thermocouple locations.

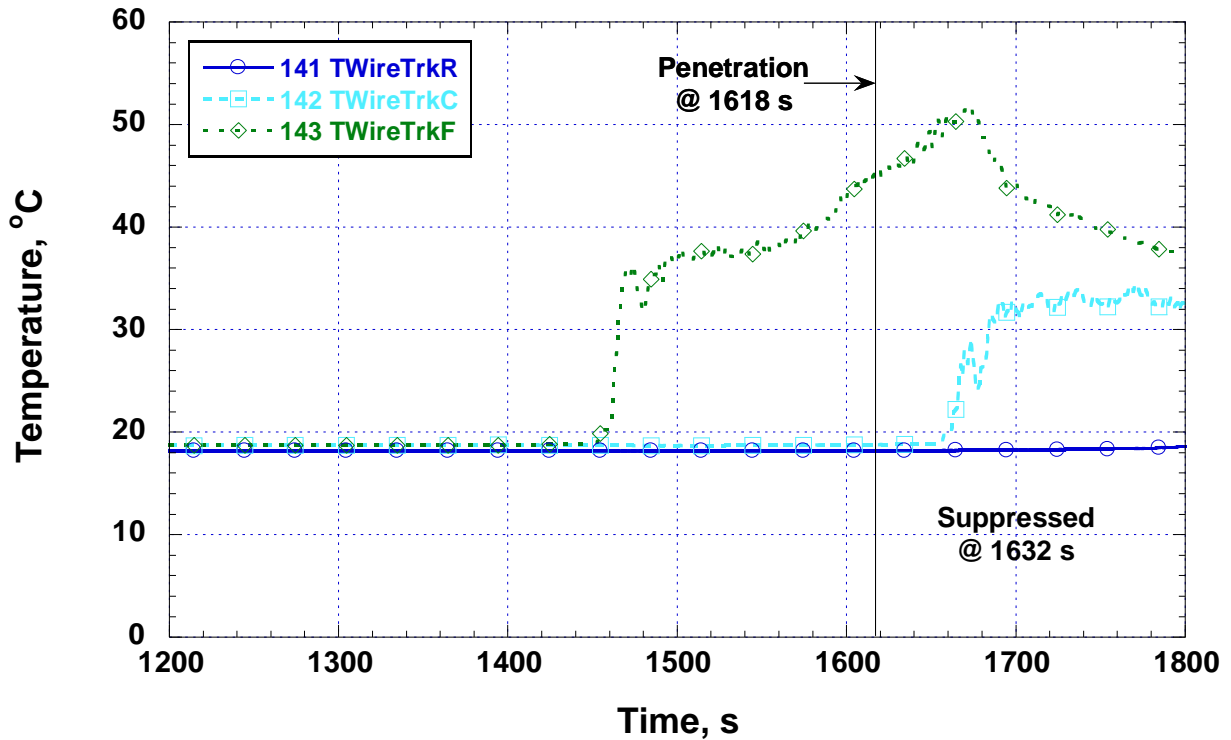


Figure 36 A plot of test 2 (drive axle) temperatures versus time for TCs inside the central tunnel for wires under the interior floor along the centerline of the coach. R, C, and F represent rear, center, and front, respectively, of the test section. Table 1 and Figure 9 describe thermocouple locations.

Axle Temperatures

Possible spread of fire along the axles and upward through the floor or to the far side tires and panels was a concern that prompted monitoring of this region. Figure 37 and Figure 38 are plots of temperature for test 1 and 2, respectively, for the thermocouples located above the two axles. In Figure 37, for the tag axle wheel heating test, both of the passenger side thermocouples over each axle showed significant heating with the tag axle at a maximum temperature of 700 °C and the drive axle maximum at 450 °C. It is surprising that the tag axle passenger side temperature reached its maximum over 2 min prior to penetration and then dropped down to 350 °C. For test 1, the center and driver's side axle temperatures barely exceeded 100 °C before penetration which indicates that along the axle to the far side was not a significant pathway for fire spread.

For test 2, Figure 38 shows the drive axle passenger side and center thermocouples rising to 950 °C and 550 °C, respectively. Even the drive axle driver's side thermocouple rose to 300 °C before penetration which is significant in that temperatures over 400 °C generally will ignite flammable materials such as the tire and GRP panels. While passenger side and center position axle temperatures greater than 550 °C were significant for causing ignition of nearby flammable materials, the interior floor and central tunnel temperatures showed very little thermal penetration. The far position rose past 300 °C at about 50 °C /min, but it is unknown whether this rate would have continued and whether flammable materials would have eventually ignited if the fire were allowed to continue.

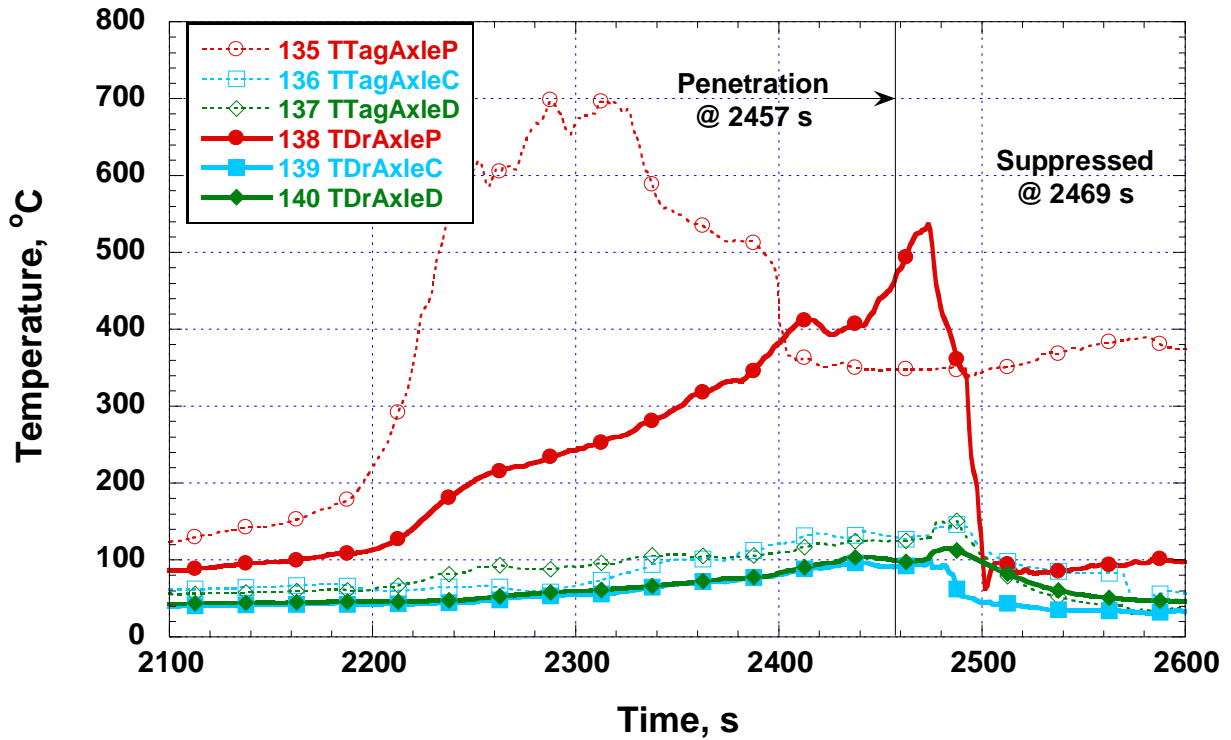


Figure 37 A plot of test 1 (tag axle) temperatures versus time for TCs above the two axles. P, C, and D represent passenger side, center, and driver side, respectively.

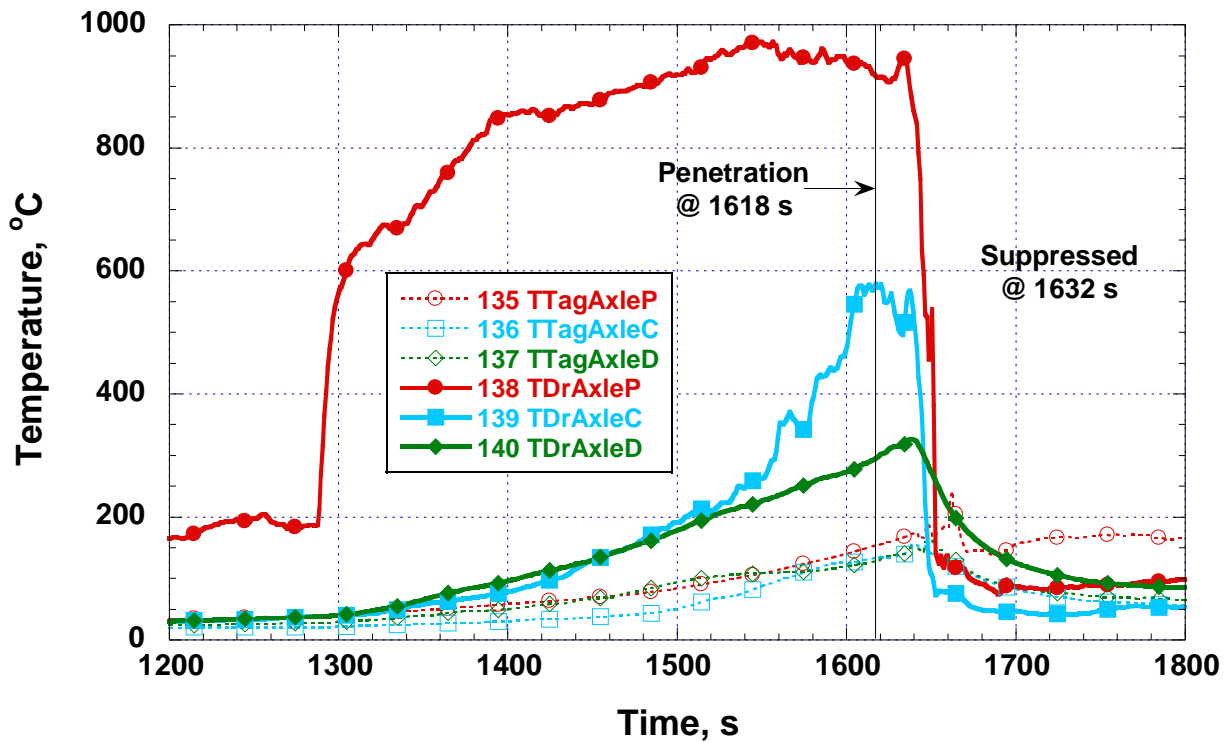


Figure 38 A plot of test 2 (drive axle) temperatures versus time for TCs above the two axles. P, C, and D represent passenger side, center, and driver side, respectively.

Heat Fluxes

Table 2 lists the locations and orientations of the heat flux gauges corresponding to the following results. Figure 39 and Figure 40 show the results of heat flux measurements for test 1 (tag axle wheel heating) and test 2 (drive axle wheel heating), respectively. For test 1, only the seat position heat flux rose significantly to about 1.5 kW/m^2 before penetration. After penetration, despite extinguishment activities, the heat flux increased to about 4 kW/m^2 . The other fluxes in test 1 remained below 0.4 kW/m^2 before penetration.

For test 2, the seat position heat flux rose to about 3 kW/m^2 before penetration and the front side facing gauge rose to 1.5 kW/m^2 . The other fluxes remained below 0.5 kW/m^2 .

The heat flux required for piloted ignition of materials such as fabric covered seat cushions is typically greater than 6 kW/m^2 . [10] The situation in these experiments was unpiloted which requires much greater heat flux for ignition so the thermal radiation through the windows was not nearly enough to ignite flammable materials inside. At the stages of growth of the tire/motorcoach fires upon window penetration, the heat fluxes were not sufficient alone to ignite the seat material before or after the window breakage. Without extinguishment, additional glass breakage/removal and further fire growth would allow greater heat fluxes on the interior materials as well as direct impingement of hot gases and flames leading to ignition by thermal radiation alone or piloted.

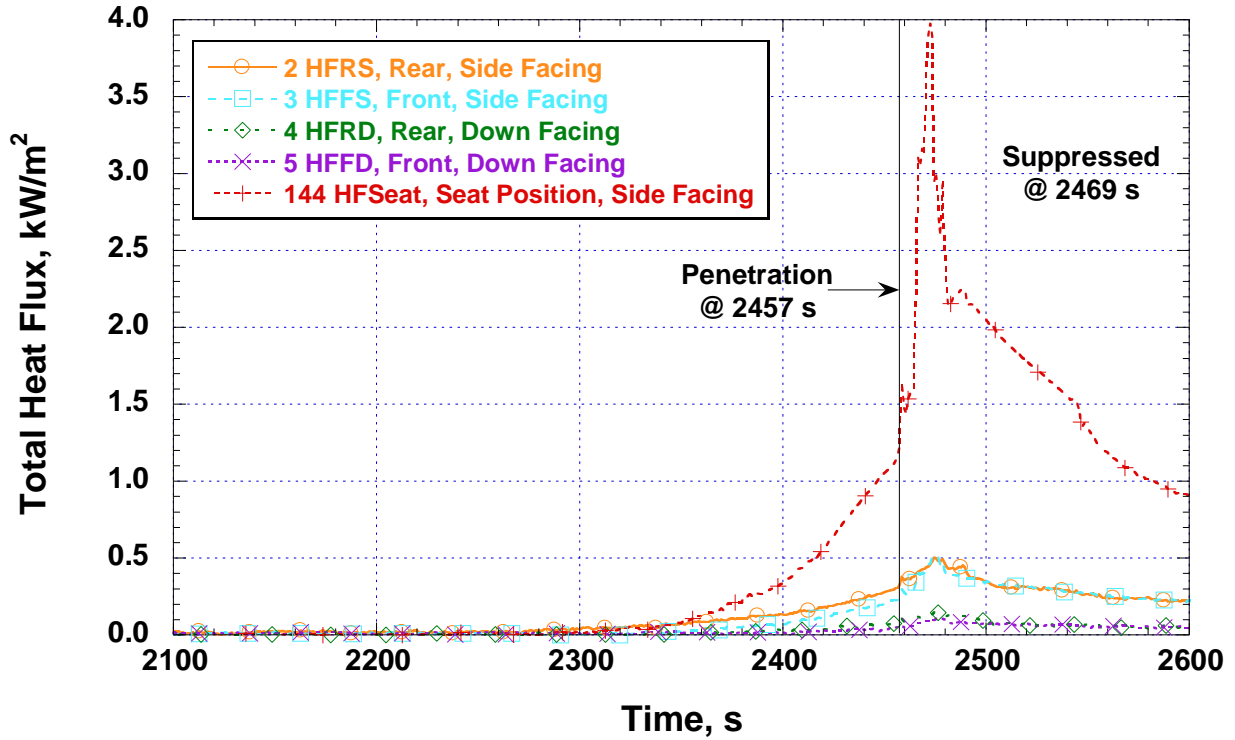


Figure 39 A plot of test 1 (tag axle) total heat flux versus time for the 5 heat flux gauges in the passenger compartment. Table 2 provides additional descriptions of the locations.

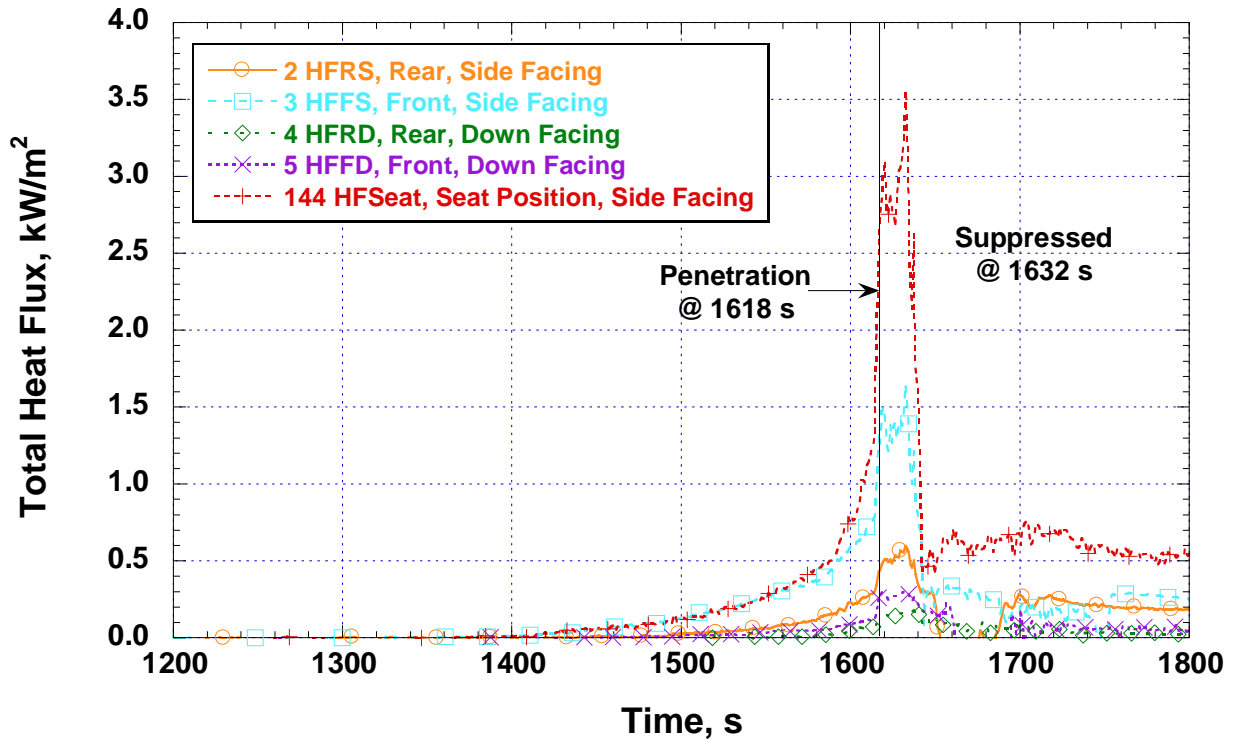


Figure 40 A plot of test 2 (drive axle) total heat flux versus time for the 5 heat flux gauges in the passenger compartment. Table 2 provides additional descriptions of the locations.

Photographs

Several hundred digital photographs were taken of the motorcoach before, during, and after testing. A select collection is shown in Appendix C.

SUMMARY AND OBSERVATIONS

Two motorcoach tire fire experiments were conducted to investigate the mode by which tire fires penetrate the passenger compartment. A novel burner was designed to simulate frictional heating by failed axle bearings, locked brakes, or dragged blown tires with localized heating of wheel metal without substantially preheating the tire rubber. Temperatures and heat fluxes were recorded along with video and still images. Based on this specific motorcoach and the conditions of these particular experiments, the following conclusions can be drawn:

- Tire fire penetration into the passenger compartment occurred from flame impingement on windows and resulting glass breakage.
- A tire fire can spread to flammable exterior fenders or panels within 2 min of a sustained fire on the tire.
- The time between the start of a self-sustained or established tire fire and window breakage by fire can be less than 5 min.
- The slow rate of rise of floor temperatures suggests that the possibility is low for fire penetrating through the floor into the main passenger compartment or lavatory within a few minutes of the window penetration.
- Based on the rates of temperature increase observed before extinguishment, there is a possibility of an initial tire fire crossing the motorcoach by way of an axle within several minutes of window penetration. Window penetration on the second side would lag behind that on the primary side by the delay of the spread of fire across the axle.
- Temperatures in the wheel well and along the axles were sufficiently high with potential to damage any flammable materials under the floor, but interior areas near the fire are protected by a layer of insulation. Additional penetration points could arise from local degradation of less protected areas, but this was not observed in these tests.
- By the relatively easy extinguishment of these tire fires (less than 15 s) with foam and water, it is apparent that these tire fires, while established, were not yet fully involved (when all tire rubber in contact with the wheel is burning simultaneously). [11] If heating of wheel metal was substantially greater for an actual moving motorcoach than it was for these experiments, it's possible that a much larger initial fire would ensue involving the whole tire when the coach stopped rolling. A tire fire which was more fully involved initially than for these tests could have a different spreading behavior which could change the timing of passenger compartment penetration.

Additional motorcoach experiments were planned to investigate the feasibility of protecting the windows from tire fire penetration. Potential protective measures included: replacing flammable materials above the tires with sheet metal, covering the flammable materials above the tires with an intumescent coating, and locating a deflector above the tires to steer the fire plume away from the side of the bus. A final experiment was planned which would explore the timing for passenger compartment tenability conditions to be reached after tire fire penetration.

Construction of a mock up of the whole motorcoach was intended for the tenability experiment.

ACKNOWLEDGEMENTS

This work was sponsored by the National Highway Traffic Safety Administration.

Thanks to Marco Fernandez and the Large Fire Laboratory staff (Matt Bundy, Laurean DeLauter, Tony Chakalis, and Doris Rinehart) for all the hard work preparing for and running this challenging experimental project. Thanks to Ed Hnetkovsky for help with the burner. We're grateful to the NIST Fire Protection Group and Roy McLane and Andrew Lock of the Fire Fighting Technology Group for providing backup suppression. Also, the NIST Plant Division is appreciated for providing crews to move our motorcoach.

NIST thanks Randy Smith and Alex Cook of Greyhound for technical advice regarding removal and replacement of motorcoach components.

REFERENCES

- [1] National Transportation Safety Board, Motorcoach fire on Interstate 45 during Hurricane Rita evacuation near Wilmer, Texas, September 23, 2005, NTSB/HAR-07/01, NTSB, Washington, DC, February 21, 2007.
- [2] N. R. Meltzer, G. J. Ayres, M. H. Truong, Motorcoach Fire Safety Analysis, Volpe National Transportation Systems Center for Federal Motor Carrier Safety Administration, Cambridge, MA, July 2009.
- [3] P. A. Hansen, Fire in Tires. Heat Release Rate and Response of Vehicles, SINTEF NBL Report STF25_A95039, SINTEF Norwegian Fire Research Laboratory, April 1995.
- [4] R. Hammarström, J. Axelsson, B. Reinicke, Fire Safety in Buses WP1 Report: Bus and Coach Fires in Sweden and Norway, SP Report 2006:26, SP Technical Research Institute of Sweden, 2006.
- [5] R. Hammarström, J. Axelsson, M. Försth, P. Johansson, B. Sundström, Bus Fire Safety, SP Report 2008:41, SP Technical Research Institute of Sweden, 2008.
- [6] R. A. Bryant, T. J. Ohlemiller, E. L. Johnsson, A. P. Hamins, B. S. Grove, W. F. Guthrie, A. Maranghides, G. W. Mulholland, The NIST 3 Megawatt Quantitative Heat Release Rate Facility, NIST Special Publication 1007, NIST, Gaithersburg, MD, December 2003.
- [7] C. Huggett, Estimation of Rate of Heat Release by Means of Oxygen Consumption Measurements, *Fire and Materials* **4** (2), 61-65 (1980).
- [8] L. G. Blevins, W. M. Pitts, Modeling of Bare and Aspirated Thermocouples in Compartment Fires, *Fire Safety Journal*, **33** Volume 33, Issue 4, November 1999, 239-259.
- [9] W. M. Pitts, A.V. Murthy, J. L. deRis, J. R. Filtz, K. Nygard; D. Smith, I. Wetterlund, Round Robin Study of Total Heat Flux Gauge Calibration at Fire Laboratories, *Fire Safety Journal*, Vol. 41, No. 6, 459-475, September 2006.
- [10] J. F. Krasny, W. J. Parker, V. Babrauskas, Fire Behavior of Upholstered Furniture and Mattresses, William Andrew Publishing, LLC, Norwich, NY (2001) 449 p.
- [11] J. P. Stensaas, H. C. Jacobsen, Testing of Different Portable Fire Extinguishers against Fires in Twin Tyres, SINTEF NBL Report NBL10 A01159, SINTEF Norwegian Fire Research Laboratory, December 2001.

APPENDICES

Appendix A. Motorcoach Flammability Testing Statement of Work (SOW)

1. DESCRIPTION OF WORK

Objectives

The objective of this project is to support the National Highway Traffic Safety Administration's (NHTSA) current effort on improving motorcoach fire safety based on the recent NTSB recommendations. The proposed research will:

- Establish an understanding of the development of a motorcoach fire and its subsequent spread into the passenger compartment.
- Evaluate and identify bench-scale material flammability test methods that are most likely to give a meaningful measure of the resistance of interior materials of motorcoach to a typical wheel-well fire.
- Determine the feasibility of establishing requirements for fire-hardening or fire resistance of motorcoach exterior components, including fuel system components.
- Assess tenability within the passenger compartment in the event of a wheel-well fire and identify potential mitigation strategies.

The proposed tasks will be completed in two years after the initial receipt of funds from NHTSA, with incremental funding from NHTSA in FY'08 and FY'09.

Background

On August 6, 2007, NHTSA published a comprehensive plan for motorcoach safety¹. The plan outlines how the agency intends to approach improvements to motorcoach safety in several areas, including flammability. The approach with regard to flammability was developed to address the following NTSB recommendations resulting from their investigation of the 2005 Wilmer, Texas motorcoach fire that resulted in 23 fatalities:

H-07-04: Develop a Federal Motor Vehicle Safety Standard to provide enhanced fire protection of the fuel system in areas of motorcoaches and buses where the system may be exposed to the effects of a fire.

H-07-05: Develop a Federal Motor Vehicle Safety Standard to provide fire-hardening of exterior fire-prone materials, such as those in areas around wheel-wells, to limit the potential for flame spread into a motorcoach or bus passenger compartment.

H-07-06: Develop detection systems to monitor the temperature of wheel-well compartments in motorcoaches and buses to provide early warning of malfunctions that could lead to fires.

¹ See Docket No. NHTSA-2007-28793.

H-07-07: Evaluate the need for a Federal Motor Vehicle Safety Standard that would require installation of fire detection and suppression systems on motorcoaches.

Since a full-scale fire test of a motorcoach is currently being planned and will be carried out by the SP Swedish National Testing and Research Institute² (SP) to study how fires in the engine compartment could spread to the passenger compartment, NIST's effort will focus only on fires that originate in the areas near the rear wheel well, and fuel lines to complement the SP studies. NIST's effort will also evaluate the current component test methods in use for vehicle flammability (e.g., FMVSS No. 302, or ECE Regulation 118) to provide a comparison of these two methods and will evaluate the applicability of other bench-scale material flammability test methods used by other federal regulatory agencies in other transportation sectors to assess material fire resistance to a typical motorcoach wheel-well fire.

Statement of Work

Task 1: Literature Review and Consultation on Wheel-Well Fires and Material Flammability Testing

This task includes a literature search and review plus consultation (including any travel to facilities that store coaches that have been involved in fires) with appropriate federal and industry "authorities" to identify the likely paths of motorcoach fires and their rate of development. Visits to motorcoach facilities will help data gathering on motorcoach structures for building the mock-ups (or a section of the motorcoach for mock-up testing), motorcoach components for testing, and the exposure of motorcoach components seen during a fire originating near the rear wheel-well. Since the NIST focus on fires originating external to the motorcoach passenger compartment will be the areas near wheel-wells and adjacent fuel system components, special attention will be given to the maximum flame temperatures, heat release rates and fire resistance of components located in those areas (e.g., tires, fuel lines, external body panels) that significantly affect fire spread into the passenger compartment.

A literature search on bench-scale material flammability test methods that are most likely to give a meaningful measure of the resistance of exterior, interior and fire barrier materials to the conditions encountered in a typical wheel-well fire will also be conducted. Currently, improvement of ECE Regulation 118 has been proposed by two European countries, Norway and Sweden (see footnote 2) to improve fire safety in buses. NIST will also examine other federal regulations (FAA, FRA, and FTA) as suggested by NHTSA and determine the applicability and/or adaptability to the existing FMVSS No. 302 test methods.

NIST will evaluate laboratory test results in order to compare the test methods of FMVSS No. 302 with the ECE Regulation 118, FAA, FRA, and FTA test methods for flammability of interior components. NHTSA will furnish the test specimens. The interior materials include seat cushion foam, cushion fabric cover, ceiling and wall linings, material used for the overhead luggage compartment, and flooring. The exterior materials include materials (e.g., fiberglass or other typical composites) for the exterior side wall panel and insulation material(s) used in the exterior panel. All the flammability tests will be conducted by a reputable certified testing

² Fire Safety in Buses, GRSG-93-15 (93rd GRSG, 23-26 October 2007, agenda item 3(d)).

laboratory. NIST will handle the logistics of the material flammability testing, manage the data collection, and interpret the test results. Based on the results of these and other larger-scale tests in this research study, NIST will assess the applicability of NHTSA's existing FMVSS No. 302 to motorcoach wheel-well fires and will determine if further studies are needed to improve or modify current FMVSS No. 302.

Task 2: Wheel-Well Mock-up Studies

Proper assessment of how a fire spreads from a wheel-well into the passenger compartment cannot be systematically performed until we know more about wheel-well fires and what affects the rate of fire development on the tires and on the components near the wheel-well. Several full-scale mock-up tire fire experiments have been conducted by SINTEF (Norwegian Fire Research Laboratory)³ using a 700 kW burner to pre-heat the tire rims and tires, but do not indicate conditions that were being mimicked or what the mock-ups were to test. However, these tests do provide some valuable information as to the heat release and propagation rates of tire fires.

NIST will conduct wheel-well mock-up studies to investigate the fire response behavior (including overall heat release rate (HRR)) of both interior and exterior components located near the motorcoach wheel-well (e.g., seats, trim, flooring, tires, fuel lines, fiberglass resin body panels, etc.). A mock-up of a motorcoach rear wheel-well, with exterior panels and a section of the passenger compartment adjacent to the wheel-well, will be built to study the fire physics pertinent to understanding the thermal penetration of a fire that originates near a wheel-well into a passenger compartment. Alternatively, a section of a motorcoach in the vicinity of a rear wheel-well may be used if it would be more cost effective than building a mock-up.

The mock-up will provide repeatable and controllable experimental conditions to test various components and fire countermeasures. Similar mock-ups have been used by SINTEF to study the response of vehicles exposed to tire fires (see footnote 3). In the SINTEF study, tire fires were simulated using a multi-nozzle propane burner that mimicked the heat release rate curve of two burning tires. Although such an approach lessens the variability of using individual tires and the toxic emissions associated with tire burning, used tires will be adopted in the present study to investigate the burning response of the components near a typical motorcoach rear wheel-well (tires, fuel lines, etc.). Actual tires provide more flexibility than propane burners in experimental planning for the other phases of the study (e.g., fire detection and fire suppression).

Task 3: Fire Tests and Countermeasure Demonstration/Assessment

Upon validation of the wheel-well mock-up and ignition source, NIST will employ the setup to explore potential countermeasures to motorcoach fires (including fire-hardening materials, fire detection, and fire suppression), and their effects on propagation of the fire into the passenger compartment. The mock-up will employ the components in a bus section near the wheel-well (including floor boards, insulation, wiring, fuel and HVAC lines, interior and exterior trim, seats and windows) to test various materials (e.g., intumescent materials) that might retard fire penetration into the interior, and possibly affect fire development rate in the interior.

³ SINTEF Reports, STF25 A95039, STF22 A98833, and NBL10 A01159.

NIST will also explore two countermeasures, fire detection and fire suppression. The wheel-well mock-up will be used to demonstrate the feasibility (proof of concept) of deploying such a system as a countermeasure to mitigate wheel-well fire hazards. The fire detection scheme will be based on off-the-shelf sensors (e.g., thermal sensors, ABS sensors). The fire suppression system will be selected based on the SINTEF study³. It should be noted that considerable development work would be needed, subsequent to a successful demonstration of detection and extinguishment, before a practical system could be deployed on production line buses.

Additionally, an assessment of tenability within the passenger compartment will be conducted (specifically carbon monoxide concentration and air temperature etc.) based on the wheel-well mock-up study. In particular, NIST will study the effects of broken windows on propagation of fire to the interior of the passenger compartment, and the estimated time scale on which conditions in the interior begin to become untenable.

It is anticipated that a full-scale fire will not be needed to demonstrate the countermeasure performance. However, to the extent that any full-scale fire demonstration test will be needed, NHTSA will make available the motorcoaches used in the recent crashworthiness and roof crush tests of motorcoaches. These motorcoaches will be transported to the NIST facilities in the study before the execution of Task 4.

Depending on the extent of fire growth during any needed full-scale tests, the NIST Large Fire Laboratory (LFL) may not be capable of containing a fire resulting from a *completely* engulfed motorcoach. In this case, alternative test sites such as the ATF Fire Research Laboratory in Beltsville, MD or the Montgomery County Fire and EMS Training Academy in Rockville, MD will be identified for consideration.

Based on the results of these tests, NIST will propose potential changes to existing fire resistance requirements for interior and exterior components, as well as potential motorcoach fire countermeasures.

Task 4: Quarterly and Final reports with recommendations to NHTSA

NIST will report the status of the study quarterly to NHTSA via teleconference, or other suitable arrangement. At the conclusion of the project, a report documenting all the findings and recommendations will be submitted to NHTSA for comments and review before public release.

2. SCHEDULE AND DELIVERABLES

Year 1

- Kickoff meeting. (Task 1) 15 days after receipt of funds (ARF)
- Literature review completed and Quarterly Review. (Tasks 1 and 4) 4 months ARF
- Wheel-well mock-up test plan developed and Quarterly Review. (Tasks 2 and 4) 6 months ARF
- Material flammability testing completed and

- Quarterly review (Task 1 and Task 4) 9 months ARF
 - Wheel-well mock-up experimental set-up built and Quarterly Review. (Tasks 2 and 4) 12 months ARF
- Year 2**
- Wheel-well mock-up tests completed (Task 2) 15 months ARF
 - Countermeasure test plan developed and Quarterly Review. (Tasks 3 and 4) 16 months ARF
 - Fire and countermeasure tests completed and Quarterly Review. (Tasks 3 and 4) 22 months ARF
 - Draft final report (Task 4) to NHTSA. 23 months ARF
 - Final report (Task 4) to NHTSA. 3 months after receipt of sponsor comments on draft

3. ESTIMATED BUDGET⁴

	Year 1	Year 2
Task 1		
Labor	\$31,360	
Travel	\$2,500	
Overhead	\$23,834	
Material flammability testing ⁵	\$10,114	
Other Objects	\$4,704	
Task 2		
Labor	\$52,800	
Overhead	\$40,128	
Construction of mock-up	\$15,000	
Other Objects	\$10,560	
NIST LFL user fees (4 weeks)	\$56,000 ⁶	
Task 3		
Labor		\$44,640
Overhead		\$33,926
Other Objects		\$8,928
NIST LFL user fees (3 weeks)		\$42,000
Task 4		
Labor		\$18,240
Overhead		\$13,862
Other Objects		\$2,736
TOTAL	\$247,000	\$164,332

⁴ Budget estimate does not include costs associated with full-scale fire test demonstration (if needed)

⁵ Conducted by an outside independent certified testing laboratory.

⁶ Depending on the progress, tests could begin in Year 1.

4. INTERFACES

Not applicable, if NIST test facilities can be used through the test series.

5. PROCUREMENTS

Procurements will be limited to experimental equipment and supplies.

6. REVIEWS AND REPORTS

NIST will prepare formal comments, presentations, documentation, and interim reports and will participate in meetings as agreed upon with the project sponsor at the kick-off meeting.

7. CONTROLS

Participation in meetings and activities beyond those identified above will be coordinated in advance with the sponsor via e-mail. Designated points of contact are as follows:

The NHTSA Principal Point of Contact:

Mr. David Sutula
Office of Crashworthiness Standards Rulemaking
NHTSA
1200 New Jersey Ave, SE
Washington, DC 20590
Tel: (202) 366-3273
david.sutula@dot.gov

NIST Principal Investigator and Technical Point of Contact (POC):

Jiann C. Yang, Ph.D.
Leader, Fire Metrology Group
Building and Fire Research Laboratory
National Institute of Standards and Technology
Gaithersburg, MD 20899
Tel: (301) 975-6662
Fax: (301) 975-4052
jiann.yang@nist.gov

NIST Financial POC:

Sharon Rinehart
Administrative Officer
Building and Fire Research Laboratory
National Institute of Standards and Technology
Gaithersburg, MD 20899
Tel: (301) 975-5876
Fax: (301) 975-4032
sharon.rinehart@nist.gov

8. REVISION

This is a new proposal. Any future unforeseen revision or modification of the SOW has to be agreed upon by both NHTSA and NIST.

9. ASSUMPTIONS AND CONSTRAINTS

This project rests upon the expertise of NIST BFRL staff members who have been working in these topic areas (automobile and railroad car fires and material flammability) for many years.

Risks identified in this project are the potential delay of project completion due to the scheduling of the NIST fire test facilities and the availability of the motorcoaches from the NHTSA crashworthiness tests.

Appendix B. Channel description and hook-up list

LFL MIDAS Hookup Sheet Instrument and Channel Description	LabView file: LFLMIDASCenterMotorCoach031709.vi	Series:	Motorcoach Fires - Johnson			Revision Date: 3/24/09			
Main Channels	Location Description	Overall Channel Number	Abbr.	MIDAS Station	Mod.	Mod. Ch. No.	Conv. Units	Wire	Gain
5 V Marker Channel	At MIDAS Center	0	5VMarker	Center	1	0	V	Cu	1
Tamb	At MIDAS Center station	1	Tamb	Center	1	1	°C	TC	100
Total Heat Flux Gauge Rear/Side (SN127848)	See Table 2	2	HFRS	Center	1	2	kW/m2	Cu	100
Total Heat Flux Gauge Front/Side (SN128324)	See Table 2	3	HFFS	Center	1	3	kW/m2	Cu	100
Total Heat Flux Gauge Rear/Down (SN128321)	See Table 2	4	HFRD	Center	1	4	kW/m2	Cu	100
Total Heat Flux Gauge Front/Down (SN127841)	See Table 2	5	HFDD	Center	1	5	kW/m2	Cu	100
Temperature of Total HF Gauge Rear/Side (SN127848)	See Table 2	6	THFRS	Center	1	6	°C	TC	100
Temperature of Total HF Gauge Front/Side (SN128324)	See Table 2	7	THFFS	Center	1	7	°C	TC	100
Temperature of Total HF Gauge Rear/Down (SN128321)	See Table 2	8	THFRD	Center	1	8	°C	TC	100
Temperature of Total HF Gauge Front/Down (SN127841)	See Table 2	9	THFFD	Center	1	9	°C	TC	100
Window Temperature Outside Tree 1 TC 1	79 cm up from bottom of glass	10	O1T1	Center	1	10	°C	TC	100
Window Temperature Outside Tree 1 TC 2	41 cm up from bottom of glass	11	O1T2	Center	1	11	°C	TC	100
Window Temperature Outside Tree 1 TC 3	3 cm up from bottom of glass	12	O1T3	Center	1	12	°C	TC	100
Window Temperature Outside Tree 1 TC 4	35 cm down from bottom of glass	13	O1T4	Center	1	13	°C	TC	100
Window Temperature Outside Tree 2 TC 1	79 cm up from bottom of glass	14	O2T1	Center	1	14	°C	TC	100
Window Temperature Outside Tree 2 TC 2	41 cm up from bottom of glass	15	O2T2	Center	1	15	°C	TC	100
Window Temperature Outside Tree 2 TC 3	3 cm up from bottom of glass	16	O2T3	Center	1	16	°C	TC	100
Window Temperature Outside Tree 2 TC 4	35 cm down from bottom of glass	17	O2T4	Center	1	17	°C	TC	100
Window Temperature Outside Tree 3 TC 1	79 cm up from bottom of glass	18	O3T1	Center	1	18	°C	TC	100
Window Temperature Outside Tree 3 TC 2	41 cm up from bottom of glass	19	O3T2	Center	1	19	°C	TC	100
Window Temperature Outside Tree 3 TC 3	3 cm up from bottom of glass	20	O3T3	Center	1	20	°C	TC	100
Window Temperature Outside Tree 3 TC 4	35 cm down from bottom of glass	21	O3T4	Center	1	21	°C	TC	100
Window Temperature Outside Tree 4 TC 1	79 cm up from bottom of glass	22	O4T1	Center	1	22	°C	TC	100
Window Temperature Outside Tree 4 TC 2	41 cm up from bottom of glass	23	O4T2	Center	1	23	°C	TC	100
Window Temperature Outside Tree 4 TC 3	3 cm up from bottom of glass	24	O4T3	Center	1	24	°C	TC	100
Window Temperature Outside Tree 4 TC 4	35 cm down from bottom of glass	25	O4T4	Center	1	25	°C	TC	100
Window Temperature Outside Tree 5 TC 1	79 cm up from bottom of glass	26	O5T1	Center	1	26	°C	TC	100
Window Temperature Outside Tree 5 TC 2	41 cm up from bottom of glass	27	O5T2	Center	1	27	°C	TC	100
Window Temperature Outside Tree 5 TC 3	3 cm up from bottom of glass	28	O5T3	Center	1	28	°C	TC	100
Window Temperature Outside Tree 5 TC 4	35 cm down from bottom of glass	29	O5T4	Center	1	29	°C	TC	100

Window Temperature Outside Tree 6 TC 1	79 cm up from bottom of glass	30	O6T1	Center	1	30	°C	TC	100
Window Temperature Outside Tree 6 TC 2	41 cm up from bottom of glass	31	O6T2	Center	1	31	°C	TC	100
Window Temperature Outside Tree 6 TC 3	3 cm up from bottom of glass	32	O6T3	Center	2	0	°C	TC	100
Window Temperature Outside Tree 6 TC 4	35 cm down from bottom of glass	33	O6T4	Center	2	1	°C	TC	100
Window Temperature Outside Tree 7 TC 1	79 cm up from bottom of glass	34	O7T1	Center	2	2	°C	TC	100
Window Temperature Outside Tree 7 TC 2	41 cm up from bottom of glass	35	O7T2	Center	2	3	°C	TC	100
Window Temperature Outside Tree 7 TC 3	3 cm up from bottom of glass	36	O7T3	Center	2	4	°C	TC	100
Window Temperature Outside Tree 7 TC 4	35 cm down from bottom of glass	37	O7T4	Center	2	5	°C	TC	100
Window Temperature Outside Tree 8 TC 1	79 cm up from bottom of glass	38	O8T1	Center	2	6	°C	TC	100
Window Temperature Outside Tree 8 TC 2	41 cm up from bottom of glass	39	O8T2	Center	2	7	°C	TC	100
Window Temperature Outside Tree 8 TC 3	3 cm up from bottom of glass	40	O8T3	Center	2	8	°C	TC	100
Window Temperature Outside Tree 8 TC 4	35 cm down from bottom of glass	41	O8T4	Center	2	9	°C	TC	100
Window Temperature Outside Tree 9 TC 1	79 cm up from bottom of glass	42	O9T1	Center	2	10	°C	TC	100
Window Temperature Outside Tree 9 TC 2	41 cm up from bottom of glass	43	O9T2	Center	2	11	°C	TC	100
Window Temperature Outside Tree 9 TC 3	3 cm up from bottom of glass	44	O9T3	Center	2	12	°C	TC	100
Window Temperature Outside Tree 9 TC 4	35 cm down from bottom of glass	45	O9T4	Center	2	13	°C	TC	100
Window Temperature Outside Tree 10 TC 1	79 cm up from bottom of glass	46	O10T1	Center	2	14	°C	TC	100
Window Temperature Outside Tree 10 TC 2	41 cm up from bottom of glass	47	O10T2	Center	2	15	°C	TC	100
Window Temperature Outside Tree 10 TC 3	3 cm up from bottom of glass	48	O10T3	Center	2	16	°C	TC	100
Window Temperature Outside Tree 10 TC 4	35 cm down from bottom of glass	49	O10T4	Center	2	17	°C	TC	100
Window Temperature Outside Tree 11 TC 1	79 cm up from bottom of glass	50	O11T1	Center	2	18	°C	TC	100
Window Temperature Outside Tree 11 TC 2	41 cm up from bottom of glass	51	O11T2	Center	2	19	°C	TC	100
Window Temperature Outside Tree 11 TC 3	3 cm up from bottom of glass	52	O11T3	Center	2	20	°C	TC	100
Window Temperature Outside Tree 11 TC 4	35 cm down from bottom of glass	53	O11T4	Center	2	21	°C	TC	100
Window Temperature Outside Tree 12 TC 1	79 cm up from bottom of glass	54	O12T1	Center	2	22	°C	TC	100
Window Temperature Outside Tree 12 TC 2	41 cm up from bottom of glass	55	O12T2	Center	2	23	°C	TC	100
Window Temperature Outside Tree 12 TC 3	3 cm up from bottom of glass	56	O12T3	Center	2	24	°C	TC	100
Window Temperature Outside Tree 12 TC 4	35 cm down from bottom of glass	57	O12T4	Center	2	25	°C	TC	100
Window Temperature Inside Tree 1 TC 0.5	17 cm above Tree1 TC1	58	I1T0	Center	2	26	°C	TC	100
Window Temperature Inside Tree 1 TC 1	79 cm up from bottom of glass	59	I1T1	Center	2	27	°C	TC	100
Window Temperature Inside Tree 1 TC 2	41 cm up from bottom of glass	60	I1T2	Center	2	28	°C	TC	100
Window Temperature Inside Tree 1 TC 3	3 cm up from bottom of glass	61	I1T3	Center	2	29	°C	TC	100
Window Temperature Inside Tree 2 TC 0.5	17 cm above Tree 2 TC1	62	I2T0	Center	2	30	°C	TC	100
Window Temperature Inside Tree 2 TC 1	79 cm up from bottom of glass	63	I2T1	Center	2	31	°C	TC	100
Window Temperature Inside Tree 2 TC 2	41 cm up from bottom of glass	64	I2T2	Center	3	0	°C	TC	100
Window Temperature Inside Tree 2 TC 3	3 cm up from bottom of glass	65	I2T3	Center	3	1	°C	TC	100
Window Temperature Inside Tree 3 TC 0.5	17 cm above Tree 3 TC1	66	I3T0	Center	3	2	°C	TC	100
Window Temperature Inside Tree 3 TC 1	79 cm up from bottom of glass	67	I3T1	Center	3	3	°C	TC	100
Window Temperature Inside Tree 3 TC 2	41 cm up from bottom of glass	68	I3T2	Center	3	4	°C	TC	100

Window Temperature Inside Tree 3 TC 3	3 cm up from bottom of glass	69	I3T3	Center	3	5	°C	TC	100
Window Temperature Inside Tree 4 TC 0.5	17 cm above Tree 4 TC1	70	I4T0	Center	3	6	°C	TC	100
Window Temperature Inside Tree 4 TC 1	79 cm up from bottom of glass	71	I4T1	Center	3	7	°C	TC	100
Window Temperature Inside Tree 4 TC 2	41 cm up from bottom of glass	72	I4T2	Center	3	8	°C	TC	100
Window Temperature Inside Tree 4 TC 3	3 cm up from bottom of glass	73	I4T3	Center	3	9	°C	TC	100
Window Temperature Inside Tree 5 TC 0.5	17 cm above Tree 5 TC1	74	I5T0	Center	3	10	°C	TC	100
Window Temperature Inside Tree 5 TC 1	79 cm up from bottom of glass	75	I5T1	Center	3	11	°C	TC	100
Window Temperature Inside Tree 5 TC 2	41 cm up from bottom of glass	76	I5T2	Center	3	12	°C	TC	100
Window Temperature Inside Tree 5 TC 3	3 cm up from bottom of glass	77	I5T3	Center	3	13	°C	TC	100
Window Temperature Inside Tree 6 TC 0.5	17 cm above Tree 6 TC1	78	I6T0	Center	3	14	°C	TC	100
Window Temperature Inside Tree 6 TC 1	79 cm up from bottom of glass	79	I6T1	Center	3	15	°C	TC	100
Window Temperature Inside Tree 6 TC 2	41 cm up from bottom of glass	80	I6T2	Center	3	16	°C	TC	100
Window Temperature Inside Tree 6 TC 3	3 cm up from bottom of glass	81	I6T3	Center	3	17	°C	TC	100
Window Temperature Inside Tree 7 TC 0.5	17 cm above Tree 7 TC1	82	I7T0	Center	3	18	°C	TC	100
Window Temperature Inside Tree 7 TC 1	79 cm up from bottom of glass	83	I7T1	Center	3	19	°C	TC	100
Window Temperature Inside Tree 7 TC 2	41 cm up from bottom of glass	84	I7T2	Center	3	20	°C	TC	100
Window Temperature Inside Tree 7 TC 3	3 cm up from bottom of glass	85	I7T3	Center	3	21	°C	TC	100
Window Temperature Inside Tree 8 TC 0.5	17 cm above Tree 8 TC1	86	I8T0	Center	3	22	°C	TC	100
Window Temperature Inside Tree 8 TC 1	79 cm up from bottom of glass	87	I8T1	Center	3	23	°C	TC	100
Window Temperature Inside Tree 8 TC 2	41 cm up from bottom of glass	88	I8T2	Center	3	24	°C	TC	100
Window Temperature Inside Tree 8 TC 3	3 cm up from bottom of glass	89	I8T3	Center	3	25	°C	TC	100
Window Temperature Inside Tree 9 TC 0.5	17 cm above Tree 9 TC1	90	I9T0	Center	3	26	°C	TC	100
Window Temperature Inside Tree 9 TC 1	79 cm up from bottom of glass	91	I9T1	Center	3	27	°C	TC	100
Window Temperature Inside Tree 9 TC 2	41 cm up from bottom of glass	92	I9T2	Center	3	28	°C	TC	100
Window Temperature Inside Tree 9 TC 3	3 cm up from bottom of glass	93	I9T3	Center	3	29	°C	TC	100
Window Temperature Inside Tree 10 TC 0.5	17 cm above Tree 10 TC1	94	I10T0	Center	3	30	°C	TC	100
Window Temperature Inside Tree 10 TC 1	79 cm up from bottom of glass	95	I10T1	Center	3	31	°C	TC	100
Window Temperature Inside Tree 10 TC 2	41 cm up from bottom of glass	96	I10T2	Center	4	0	°C	TC	100
Window Temperature Inside Tree 10 TC 3	3 cm up from bottom of glass	97	I10T3	Center	4	1	°C	TC	100
Window Temperature Inside Tree 11 TC 0.5	17 cm above Tree 11 TC1	98	I11T0	Center	4	2	°C	TC	100
Window Temperature Inside Tree 11 TC 1	79 cm up from bottom of glass	99	I11T1	Center	4	3	°C	TC	100
Window Temperature Inside Tree 11 TC 2	41 cm up from bottom of glass	100	I11T2	Center	4	4	°C	TC	100
Window Temperature Inside Tree 11 TC 3	3 cm up from bottom of glass	101	I11T3	Center	4	5	°C	TC	100
Window Temperature Inside Tree 12 TC 0.5	17 cm above Tree 12 TC1	102	I12T0	Center	4	6	°C	TC	100
Window Temperature Inside Tree 12 TC 1	79 cm up from bottom of glass	103	I12T1	Center	4	7	°C	TC	100
Window Temperature Inside Tree 12 TC 2	41 cm up from bottom of glass	104	I12T2	Center	4	8	°C	TC	100
Window Temperature Inside Tree 12 TC 3	3 cm up from bottom of glass	105	I12T3	Center	4	9	°C	TC	100
Inside Ignited Wheel Screwed On Back 12 o'clock Position	0° position facing outside of wheel	106	TIWh12	Center	4	10	°C	TC	100
Inside Ignited Wheel Screwed On Back 3 o'clock Position	90° position facing outside of wheel	107	TIWh3	Center	4	11	°C	TC	100

Inside Ignited Wheel Screwed On Back 6 o'clock Position	180° position facing outside of wheel	108	TIWh6	Center	4	12	°C	TC	100
Inside Ignited Wheel Screwed On Back 9 o'clock Position	270° position facing outside of wheel	109	TIWh9	Center	4	13	°C	TC	100
At Wheel/Tire Interface of Ignited Tire 12 o'clock Position	0° position facing outside of tire	110	TITi12	Center	4	14	°C	TC	100
At Wheel/Tire Interface of Ignited Tire 3 o'clock Position	90° position facing outside of tire	111	TITi3	Center	4	15	°C	TC	100
At Wheel/Tire Interface of Ignited Tire 6 o'clock Position	180° position facing outside of tire	112	TITi6	Center	4	16	°C	TC	100
At Wheel/Tire Interface of Ignited Tire 9 o'clock Position	270° position facing outside of tire	113	TITi9	Center	4	17	°C	TC	100
Inside Non-Ignited Wheels (Ignition Side) Taped On Back 12 o'clock Position	NOT USED	114	TNWh12	Center	4	18	°C	TC	100
At Wheel/Tire Interface of Non-Ignited Tire (Ignition Side)	NOT USED	115	TNTi12	Center	4	19	°C	TC	100
Inside the Wheel Well Above the Tires (Ignition Side) Behind Rear Tire		116	TIWWRear	Center	4	20	°C	TC	100
Inside the Wheel Well Above the Tires (Ignition Side) Rear Tire Center		117	TIWWRearC	Center	4	21	°C	TC	100
Inside the Wheel Well Above the Tires (Ignition Side) Middle		118	TIWWMid	Center	4	22	°C	TC	100
Inside the Wheel Well Above the Tires (Ignition Side) Front Tire Center		119	TIWWFrontC	Center	4	23	°C	TC	100
Inside the Wheel Well Above the Tires (Ignition Side) In Front of Front Tire		120	TIWWFront	Center	4	24	°C	TC	100
At Rear Wheel/Tire Interface (Unignited Side) 12 o'clock Position	NOT USED	121	TURTi12	Center	4	25	°C	TC	100
At Front Wheel/Tire Interface (Unignited Side) 12 o'clock Position	NOT USED	122	TUFTi12	Center	4	26	°C	TC	100
Inside the Wheel Well Above the Tires (Unignited Side) Rear Tire Center		123	TUWWRearC	Center	4	27	°C	TC	100
Inside the Wheel Well Above the Tires (Unignited Side) Front Tire Center		124	TUWWFrontC	Center	4	28	°C	TC	100
Joint of Floor with Lavatory Near Tank, Outside Corner of Outside Wall and Lavatory Wall		125	TLXWallCorn	Center	4	29	°C	TC	100
Joint of Floor with Lavatory Near Tank, Inside Joint of Lavatory Wall and Floor		126	TLMidJoint	Center	4	30	°C	TC	100
Joint of Floor with Lavatory Near Tank, Rear Joint Inside Lavatory of Outside Wall and Lavatory Wall		127	TLXWallJoint	Center	4	31	°C	TC	100
Along Floor Joint With Wall Above Tires 46 cm Next TC	46 cm rearward of TFWWRear	128	TFWWRear46	Center	5	0	°C	TC	100
Along Floor Joint With Wall Above Tires Behind Rear Tire	aligned over wheel well TC TIWWRear	129	TFWWRear	Center	5	1	°C	TC	100
Along Floor Joint With Wall Above Tires Rear Tire Center	aligned over wheel well TC TIWWRearC	130	TFWWRearC	Center	5	2	°C	TC	100
Along Floor Joint With Wall Above Tires Middle of Tires	aligned over wheel well TC TIWWMid	131	TFWWMid	Center	5	3	°C	TC	100
Along Floor Joint With Wall Above Tires Front Tire Center	aligned over wheel well TC TIWWFrontC	132	TFWWFrontC	Center	5	4	°C	TC	100
Along Floor Joint With Wall Above Tires in Front of Front Tire	aligned over wheel well TC TIWWFront	133	TFWWFront	Center	5	5	°C	TC	100
Along Floor Joint With Wall Above Tires 46 cm in Front	46 cm forward of TFWWFront	134	TFWWFront4	Center	5	6	°C	TC	100

of Previous TC			6						
Horizontal Rake Along Tag Axle Passenger Side		135	TTagAxleP	Center	5	7	°C	TC	100
Horizontal Rake Along Tag Axle Bus Center		136	TTagAxleC	Center	5	8	°C	TC	100
Horizontal Rake Along Tag Axle Driver's Side		137	TTagAxleD	Center	5	9	°C	TC	100
Horizontal Rake Along Drive Axle Passenger Side		138	TDrAxleP	Center	5	10	°C	TC	100
Horizontal Rake Along Drive Axle Bus Center		139	TDrAxleC	Center	5	11	°C	TC	100
Horizontal Rake Along Drive Axle Driver's Side		140	TDrAxleD	Center	5	12	°C	TC	100
Inside Central Tunnel Wiring/ Fuel Line Track Behind Rear Tires	align w/wheel well TCs	141	TWireTrkR	Center	5	13	°C	TC	100
Inside Central Tunnel Wiring/ Fuel Line Track Middle of Tires	align w/wheel well TCs	142	TWireTrkC	Center	5	14	°C	TC	100
Inside Central Tunnel Wiring/ Fuel Line Track In Front of Drive Axle	align w/wheel well TCs	143	TWireTrkF	Center	5	15	°C	TC	100
Total Heat Flux Gauge Seat (SN127842)	See Table 2	144	HFSeat	Center	5	16	kW/m2	Cu	100
Temperature of Total Heat Flux Gauge Seat (SN127842)	See Table 2	145	THFSeat	Center	5	17	°C	TC	100
Smoke Detector 1	Only used for overnight monitoring	146	SM1	Center	5	18	V	Cu	1
Smoke Detector 2	Only used for overnight monitoring	147	SM2	Center	5	19	V	Cu	1
Extra TC Temperature 1		148	TX1	Center	5	20	°C	TC	100
Extra TC Temperature 2		149	TX2	Center	5	21	°C	TC	100
Extra TC Temperature 3		150	TX3	Center	5	22	°C	TC	100
Extra TC Temperature 4		151	TX4	Center	5	23	°C	TC	100
Created Channels									
Event Marker 1		152	Event1	Center					
Event Marker 2		153	Event2	Center					

Appendix C. Photographs



Figure 41 Tag axle wheel heating experiment showing burner, shield, melted hub, and early thermal damage to tire.



Figure 42 Tag axle wheel heating experiment about 1 min after the burner was removed. The fender is already burning and the exterior panel is just igniting.



Figure 43 Tag axle wheel heating experiment about 2 min after the burner was removed. The exterior panel is burning up to the windows.



Figure 44 Tag axle wheel heating experiment about 2.5 minutes after the burner was removed showing the large quantity of black smoke on the far (driver's) side of the motorcoach.



Figure 45 Tag axle wheel heating experiment just under 4 min after the burner was removed.



Figure 46 Tag axle wheel heating experiment at fire penetration.



Figure 47 Exterior fire damage due to tag axle wheel heating experiment



Figure 48 Exterior view of window damage after tag axle wheel heating experiment.



Figure 49 Interior view of window damage after tag axle wheel heating experiment.



Figure 50 Damage to wall behind exterior panel after tag axle wheel heating experiment.



Figure 51 Damage to back side of exterior panel showing little penetration of fire through the GRP.



Figure 52 Motorcoach ready for start of drive axle wheel heating experiment.



Figure 53 Positioning of burner for drive axle wheel heating experiment.

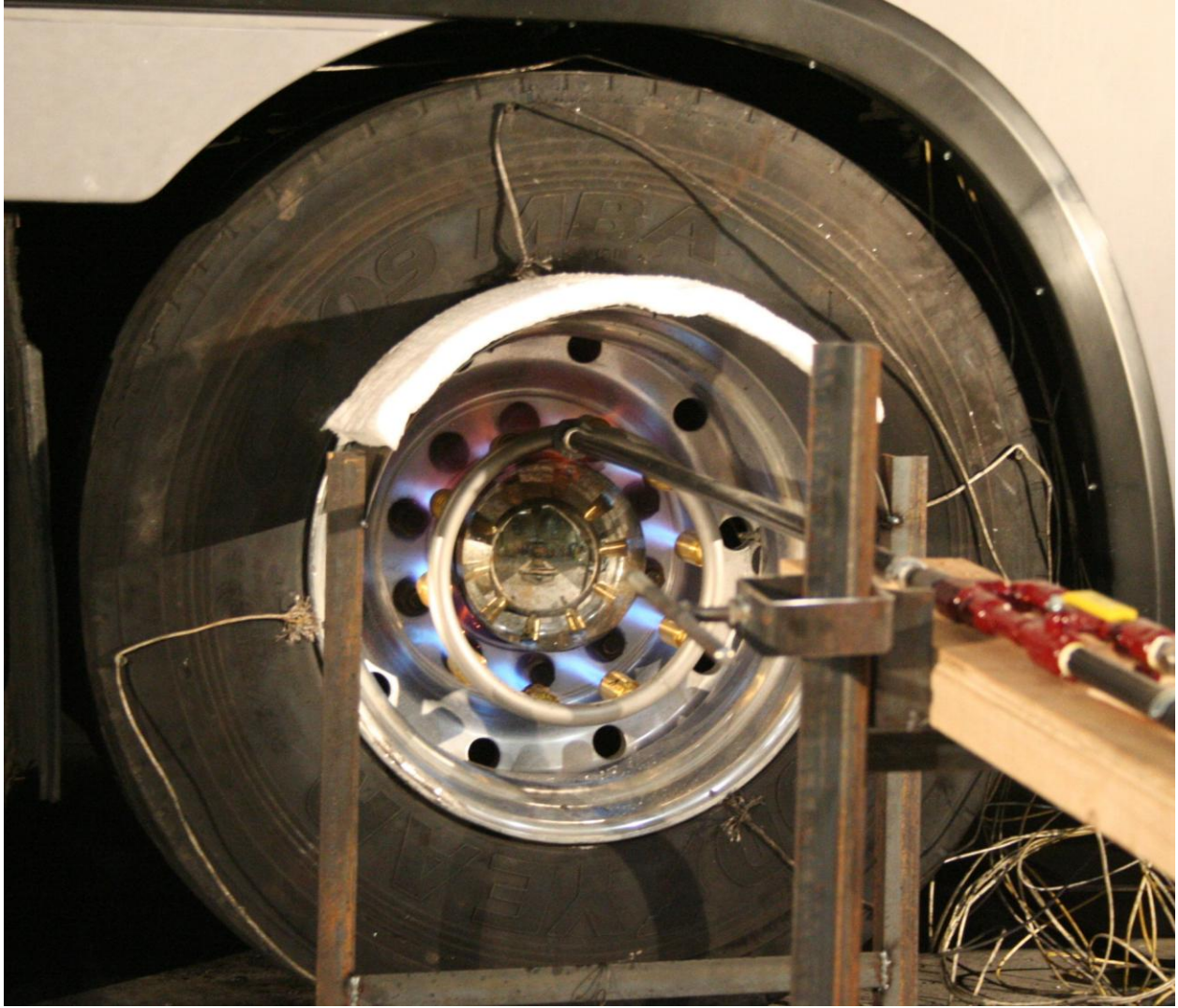


Figure 54 Close up view of burner near beginning of drive axle wheel heating experiment.



Figure 55 Drive axle wheel heating experiment about 1 min before burner was turned off.



Figure 56 Drive axle wheel heating experiment just after burner was turned off.



Figure 57 Drive axle wheel heating experiment about 30 s after burner was turned off.



Figure 58 Drive axle wheel heating experiment showing smoke coming from the external air vents.



Figure 59 Drive axle wheel heating experiment just over 1 min after burner was removed.



Figure 60 Drive axle wheel heating experiment showing fire spreading from the drive axle to the tag axle area of the fender.



Figure 61 Drive axle wheel heating experiment about 3 min after the burner was removed showing a view of the fire plume from the interior.



Figure 62 Drive axle wheel heating experiment showing large fire plumes on each tire.



Figure 63 Drive axle wheel heating experiment showing large fire plumes on each tire.



Figure 64 Drive axle wheel heating experiment showing smoke on driver's side 4 min after burner removed.



Figure 65 Drive axle wheel heating experiment showing the joined fire plumes within 2 min of fire penetration.



Figure 66 Drive axle wheel heating experiment just under 5 min after burner removal.



Figure 67 Drive axle wheel heating experiment at fire penetration. Window breakage occurred on the more rearward window while the burning tire was fairly centered on post 3 between windows.



Figure 68 Drive axle wheel heating experiment within a few seconds of fire penetration and at the very beginning of extinguishment.



Figure 69 Interior view of damage to the window over the tag axle after the drive axle wheel heating experiment fire.



Figure 70 Interior view of damage to the window over the drive axle after the drive axle wheel heating experiment fire.